

Computer Engineered 2D Materials: *Host for Unconventional Properties*

Tanusri Saha-Dasgupta

t.sahadasgupta@gmail.com

**S. N. Bose National Centre for Basic Sciences,
Kolkata, India**



Players:



Koushik Pradhan (SNB)

Rajdeep Biswas (SNB)

**Shiladitya Karmakar
(SNB -> Czech Academy of
Sciences)**

**Prabuddha Sanyal
(MAKUT)**

Acknowledgement:

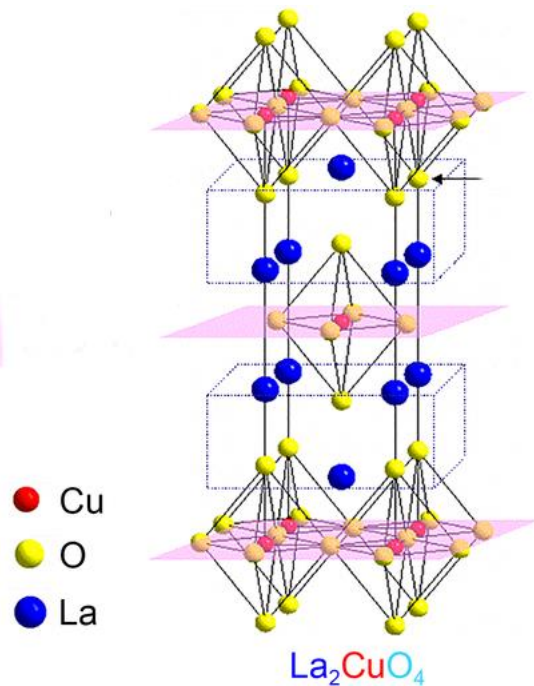


**Saumya Mukherjee
(Diamond light source)**

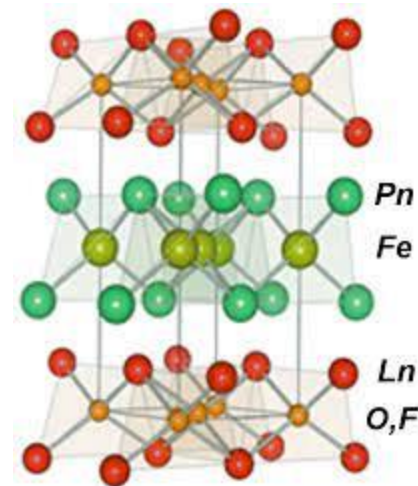
PART I

**Robust Half-metallicity and Topological Properties in
square-net Potassium Manganese Chalcogenides**

Square Net Geometries



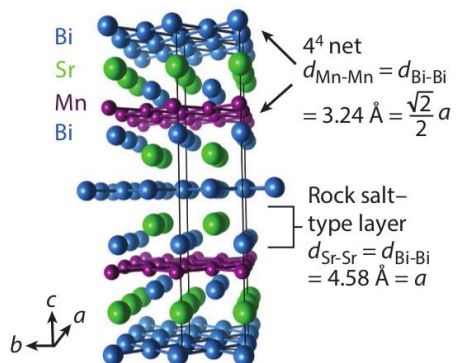
Cuprates



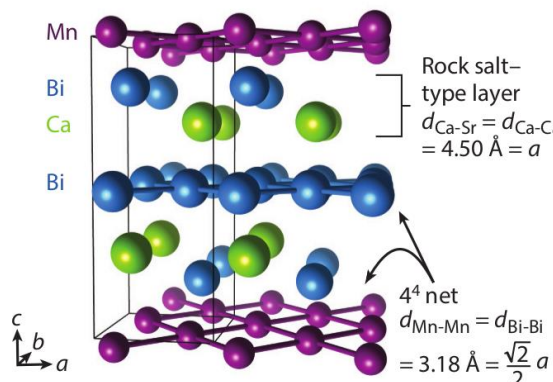
Iron pnictides

Square-Net Topological Semimetals

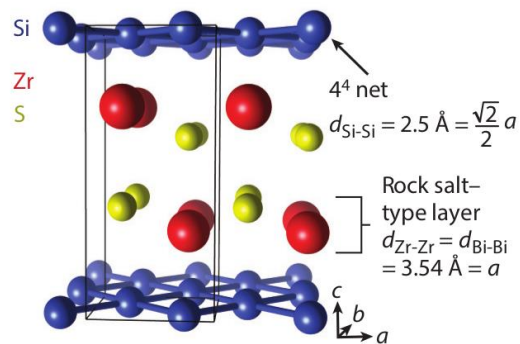
a SrMnBi_2 ($I4/mmm$)



b CaMnBi_2 ($P4/nmm$)

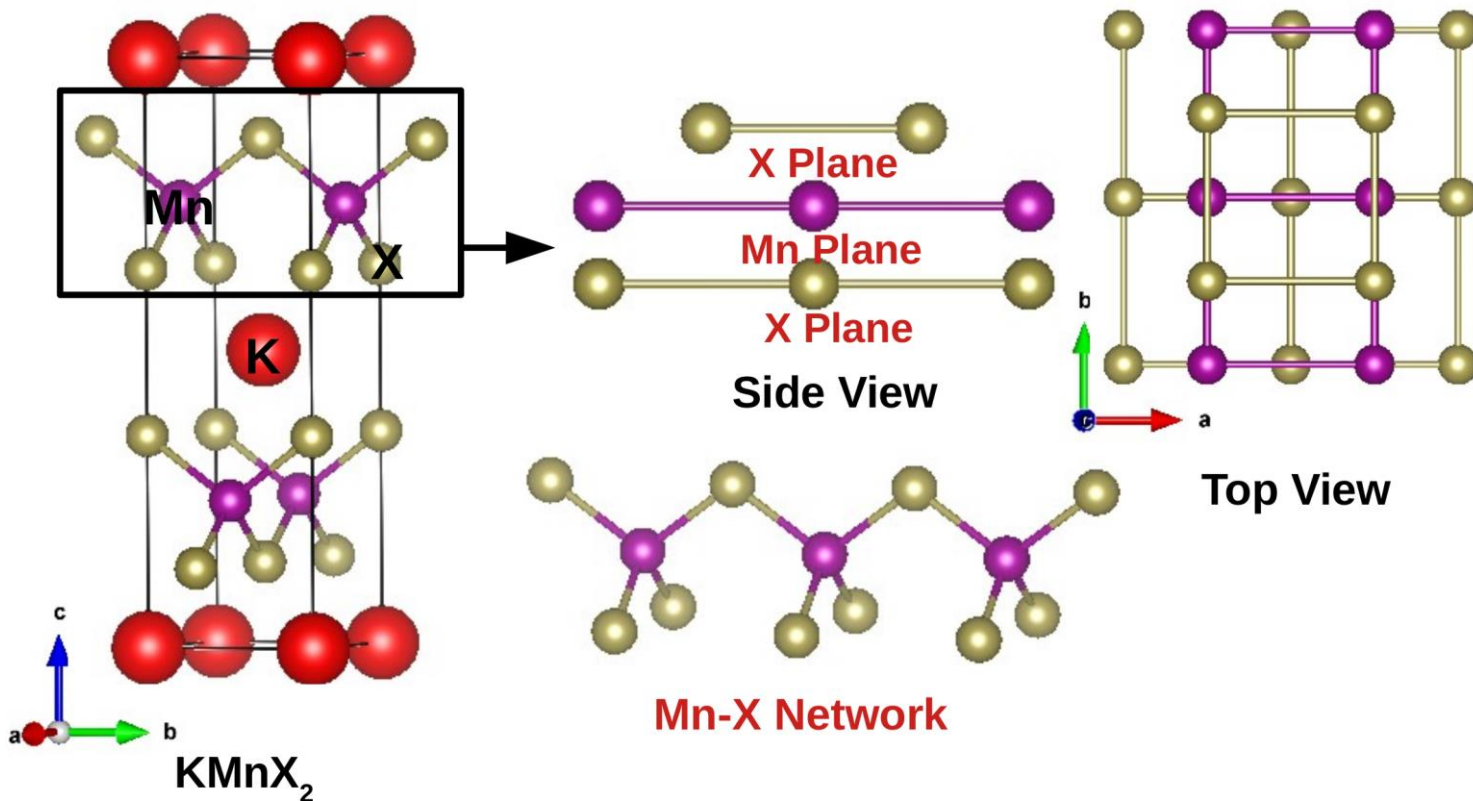


c ZrSiS ($P4/nmm$)



KMnX₂

Structure



(X)	
8	
O	2s ² 2p
15.9994	4
16	3s ² 3p
S	4
32.064	
34	4s ² 4p
Se	4
78.96	
52	5s ² 5p
Te	4
127.60	

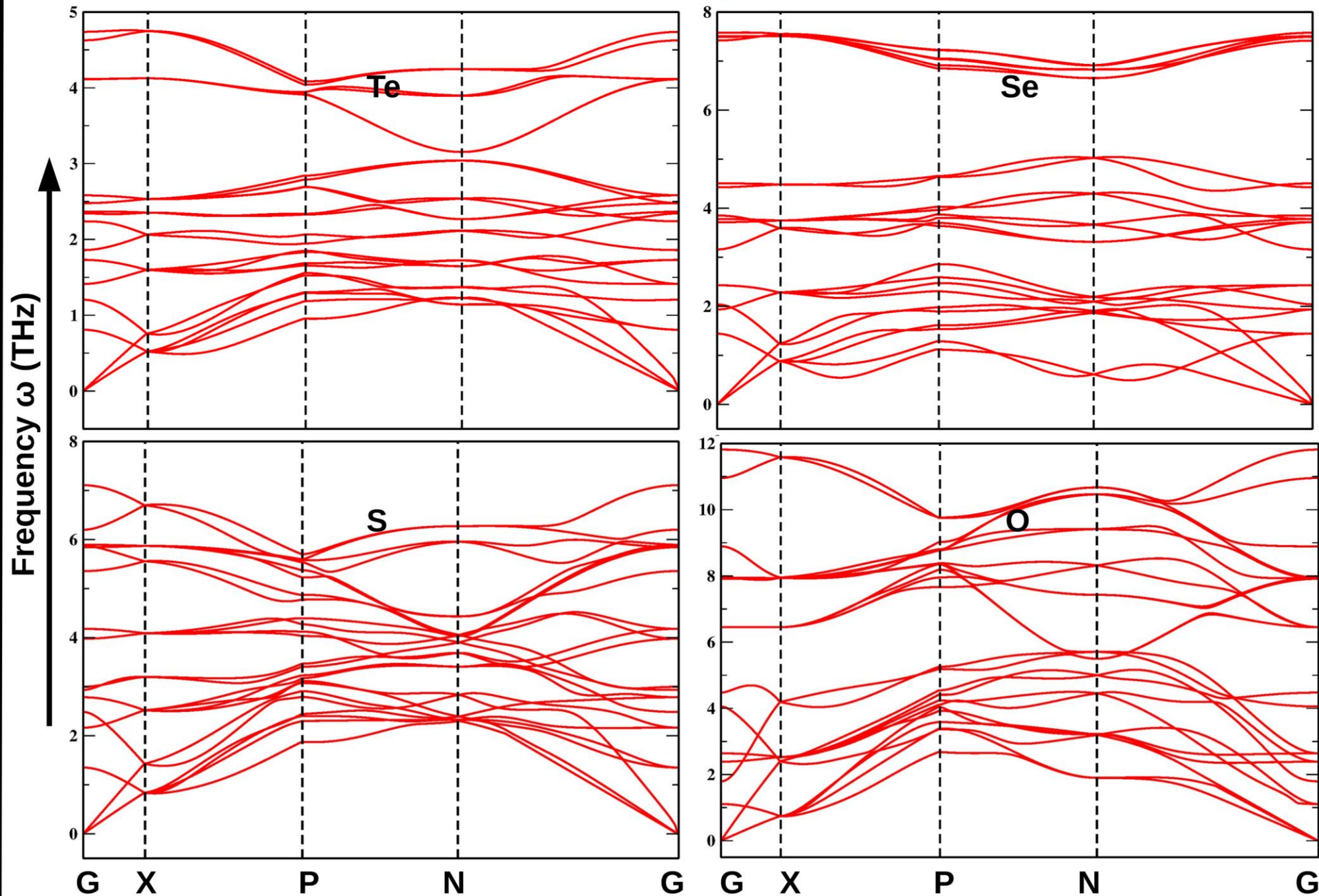
The **ternary manganese chalcogenide** having chemical composition **KMnX₂** crystallize in a **tetragonal structure**, space group **I-4m2 (No.119)**, with **two formula units** per unit cell (Z=2).

Synthesis and Structures of New Layered Ternary Manganese Selenides: **AMnSe₂** (A=Li, Na, K, Rb, Cs) and **Na₂Mn₂Se₃**

Synthesis and Structures of New Layered Ternary Manganese Tellurides: **AMnTe₂** (A = K, Rb, Cs), **Na₃Mn₄Te₆**, and **NaMn_{1.56}Te₂**

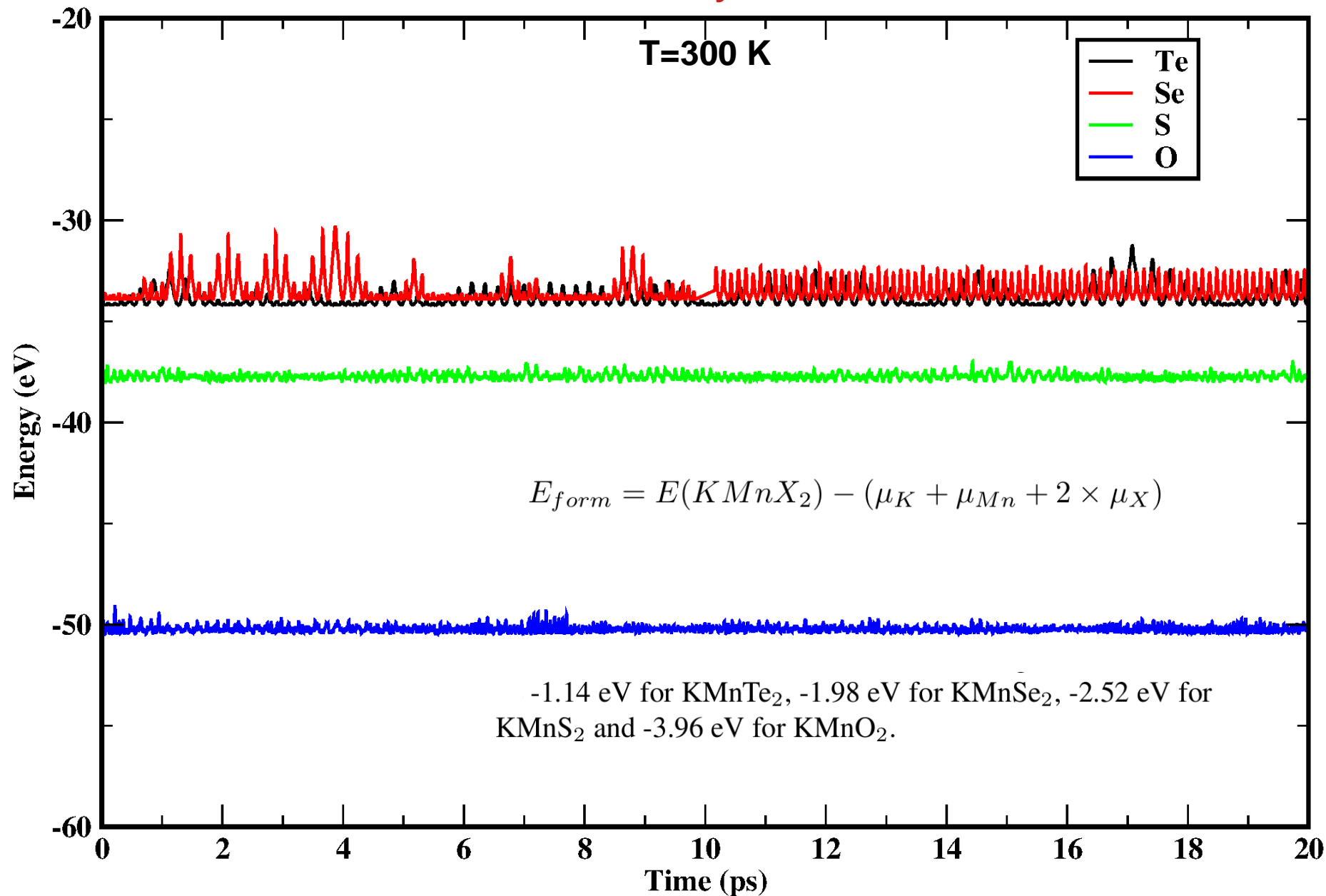
Inorg. Chem. 1999, 38, 2, 235-242

Phonon Dispersion



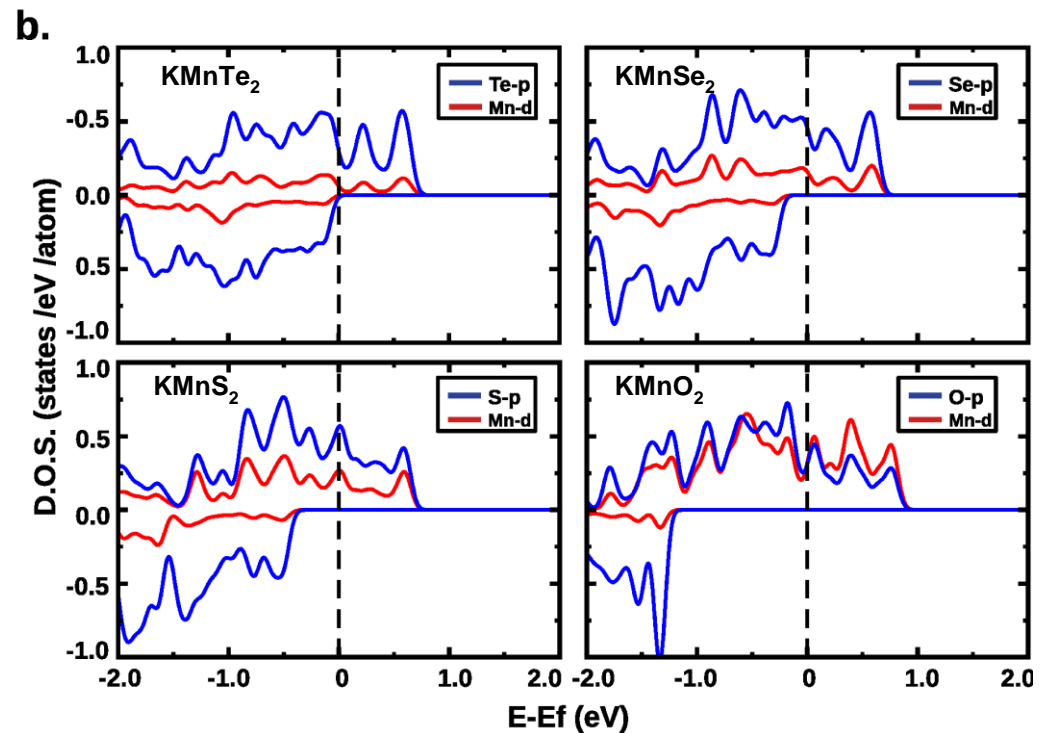
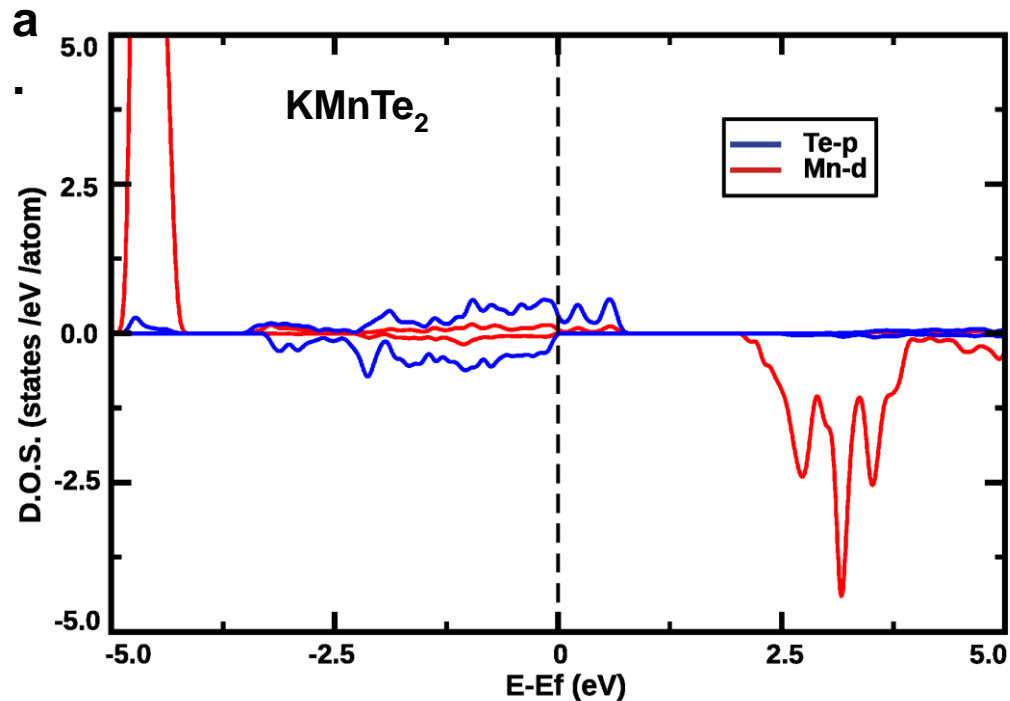
all the structures are dynamically stable

Ab initio Molecular Dynamics Simulation



➤ All the structures are thermodynamically stable.

Spin-polarized Density of States

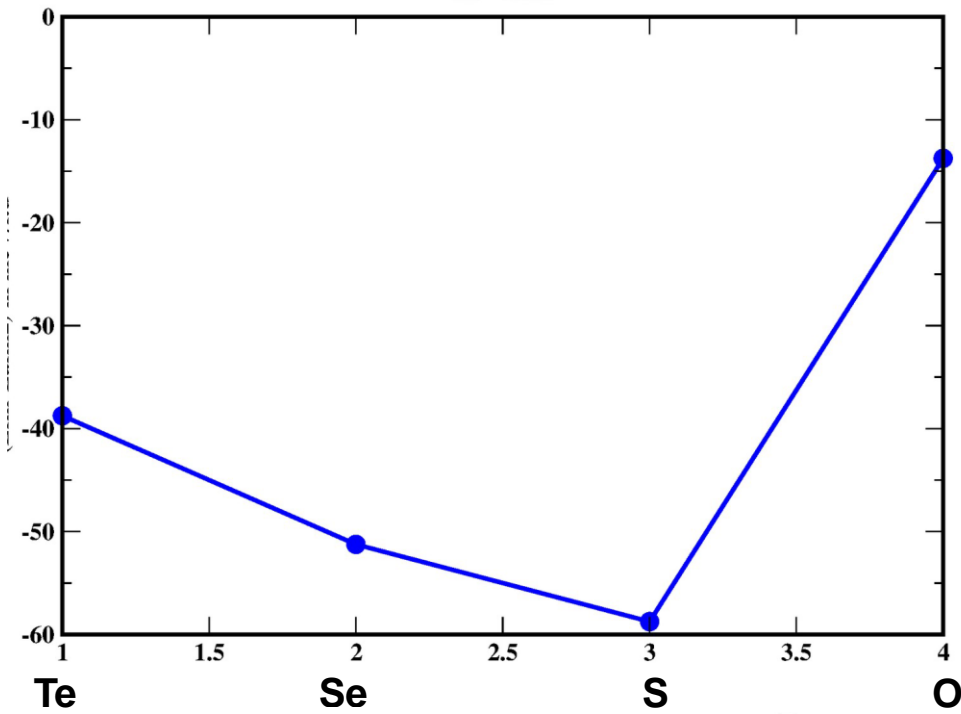


- Mn-d states are mostly occupied in the majority spin channel and empty in the minority spin channel, suggestive of a **counter intuitive Mn²⁺ nominal valence with d⁵ occupancy**.
- **In contrast to the essentially non-magnetic nature of X²⁻ anions, the X-p states are found to be strongly spin split, dominating the half-metallic electronic structure close to E_f.**
- **The dominance of low-energy X-p states over Mn-d states progressively decreases as one moves from Te to Se to S to O.**

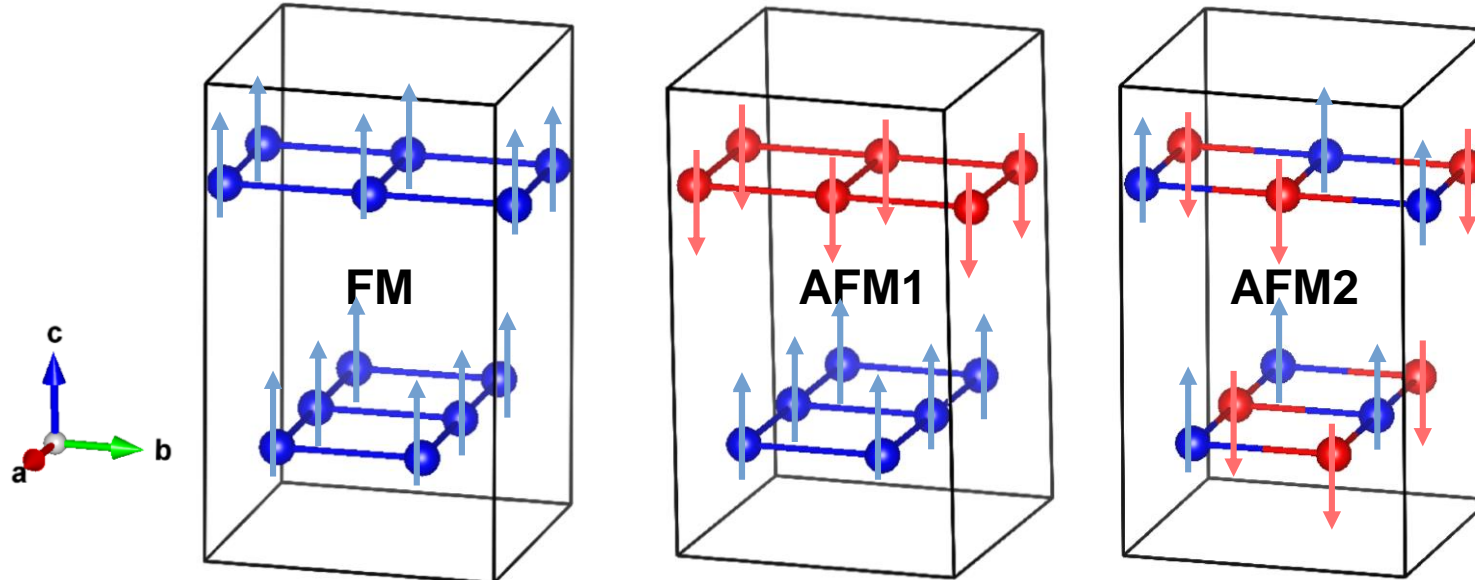
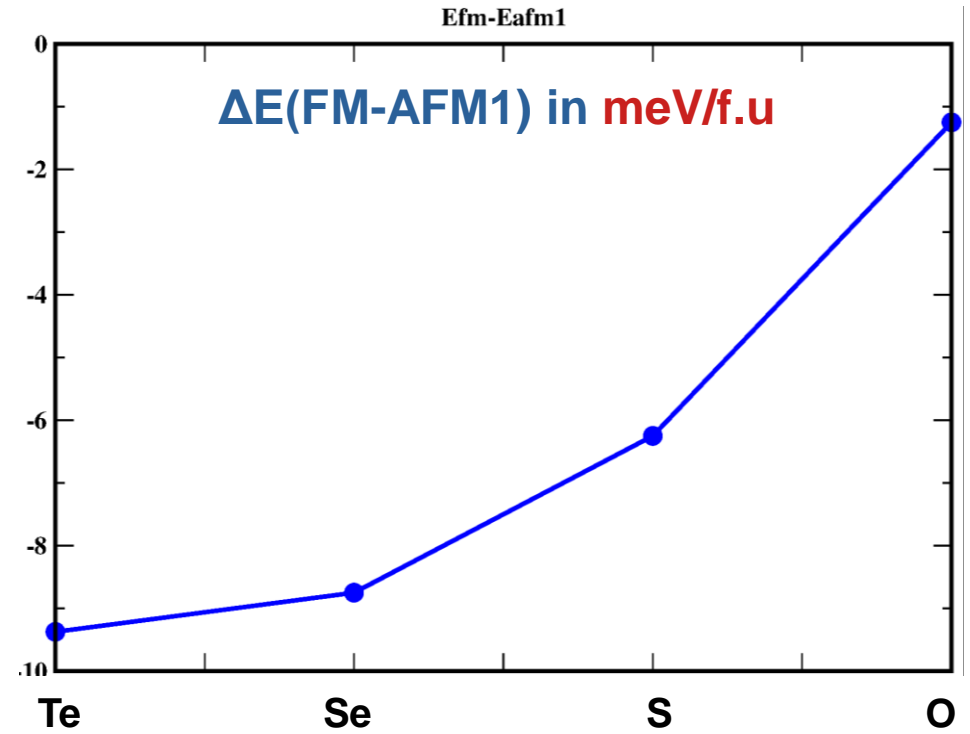
MAGNETISM

PBE+U Energy Difference (U= 5 eV J= 0.8 eV)

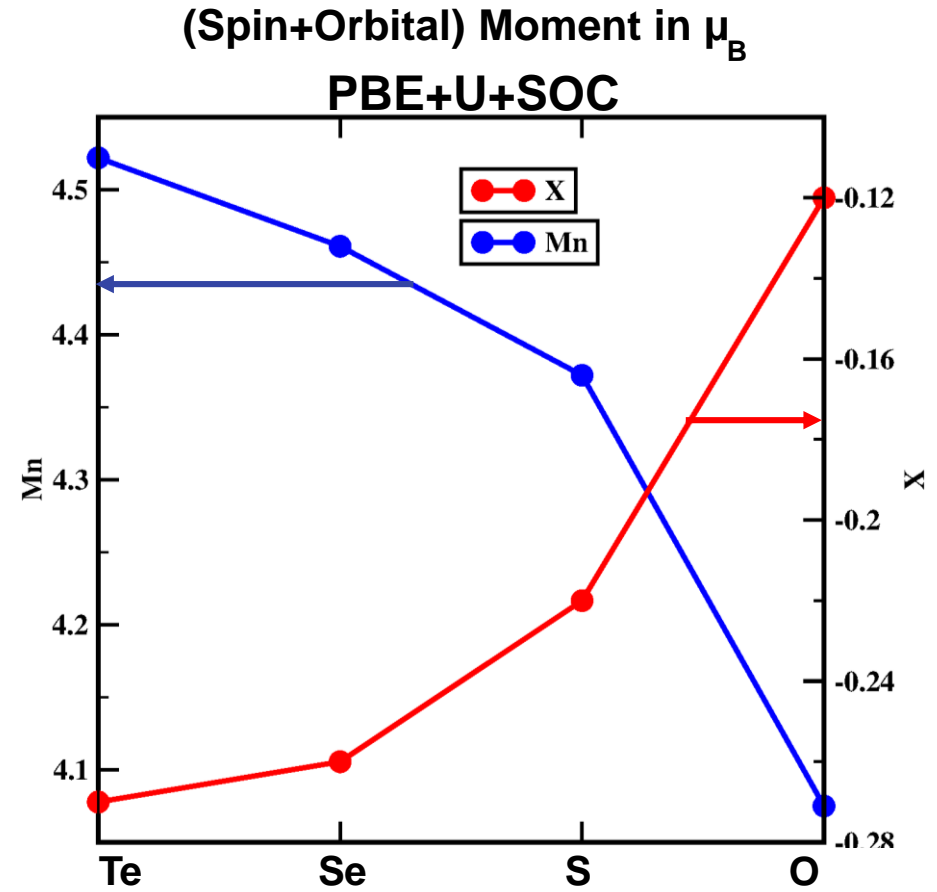
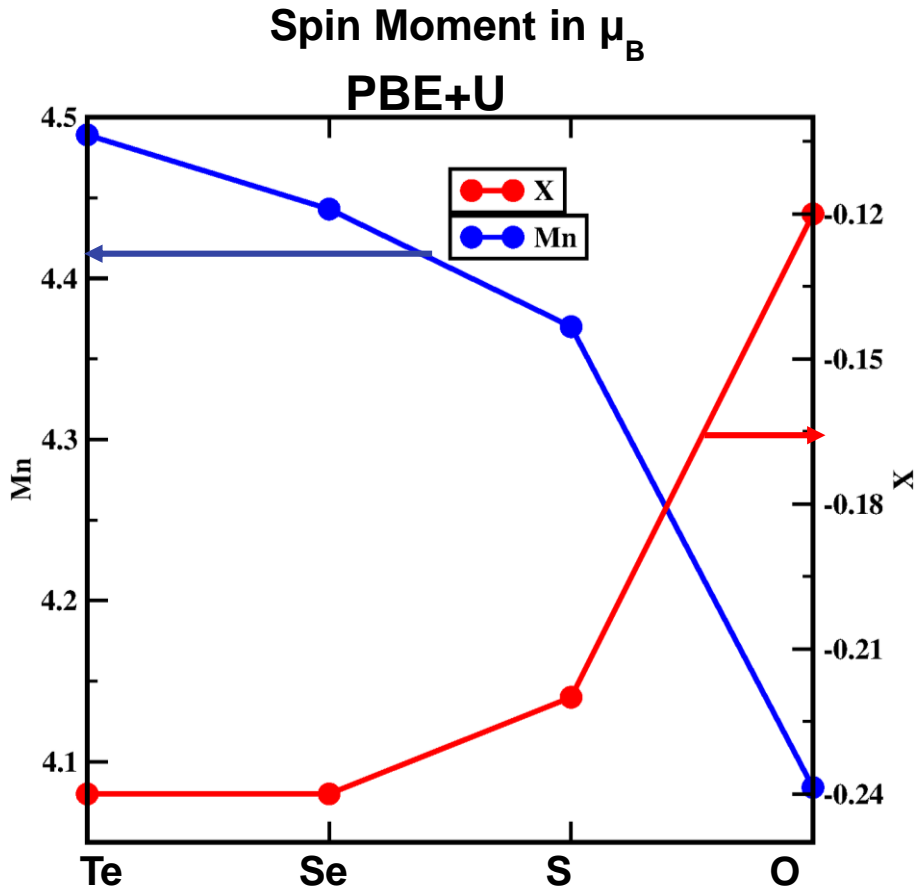
$\Delta E(\text{FM-AFM2})$ in meV/f.u



$\Delta E(\text{FM-AFM1})$ in meV/f.u



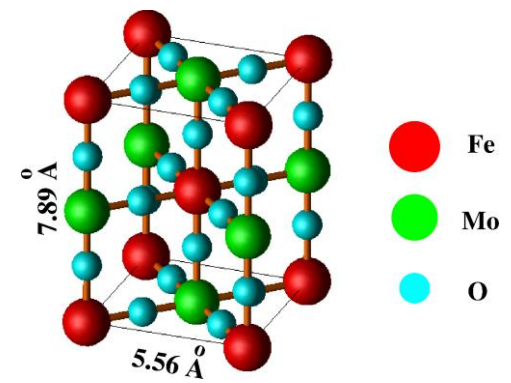
MAG. Moment
PBE+U U= 5 eV, J = 0.8 eV



- The moment of Mn and X are opposite!
- Mn should have moment $4\mu_B$ (d^4), but Mn has an average moment significantly larger than $4\mu_B$ for Te, Se and S compounds. Also Te, Se, S have significant moment, **opposite to that of Mn**.
- There are ligand holes in KMnX_2 . The ligand hole is prominent for Te, Se and S compounds.

MECHANISM OF MAGNETISM – KINETIC
ENERGY DRIVEN TWO SITE DOUBLE
EXCHANGE

SR_2FEMOO_6



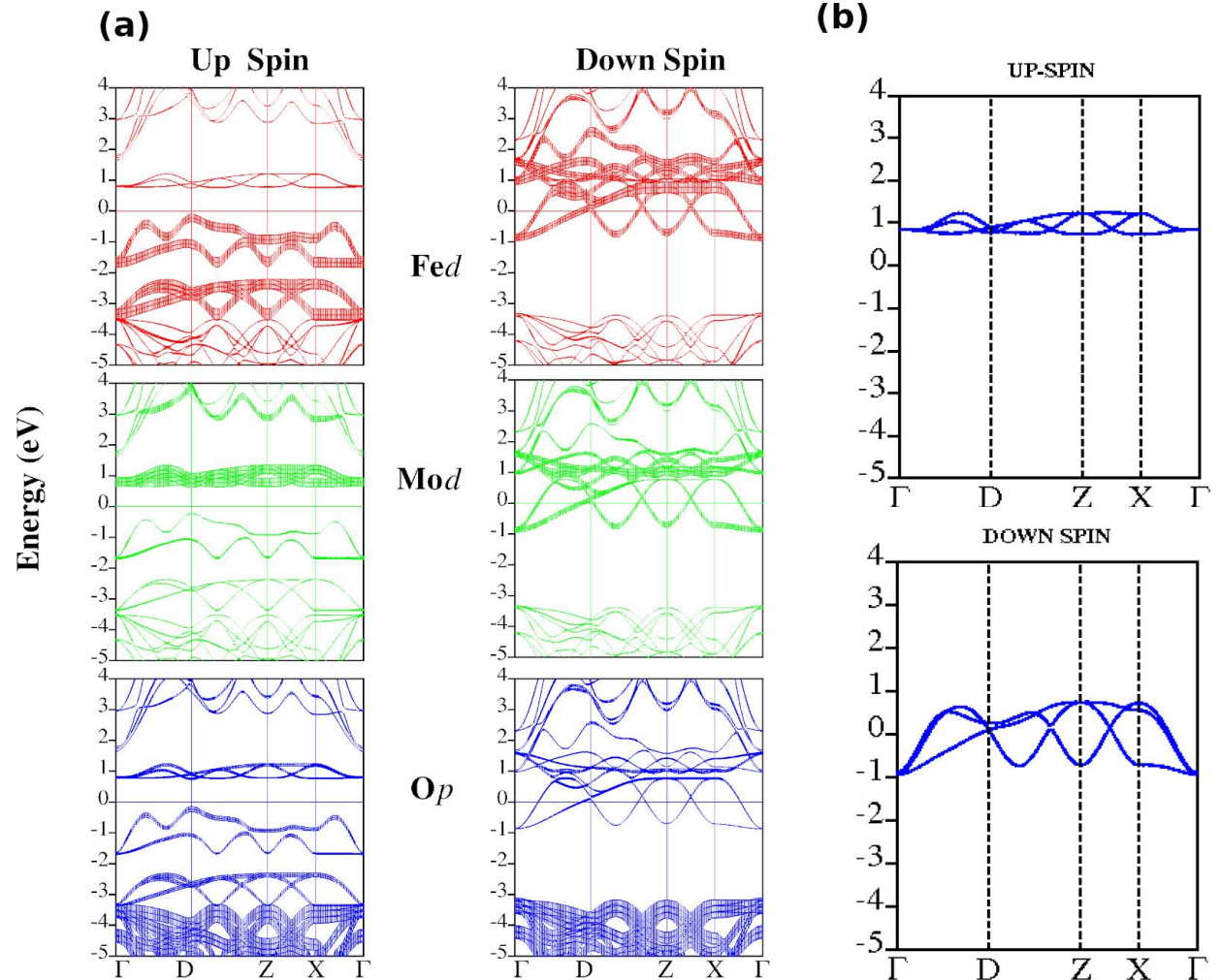
□ Half-metallic FM with $T_c \sim 450 \text{ K}$

□ Large T_c point to large inter-atomic exchange coupling

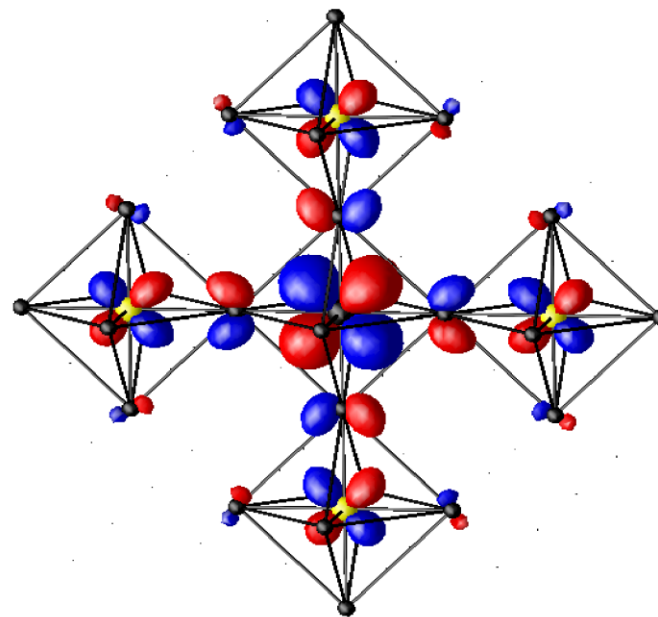
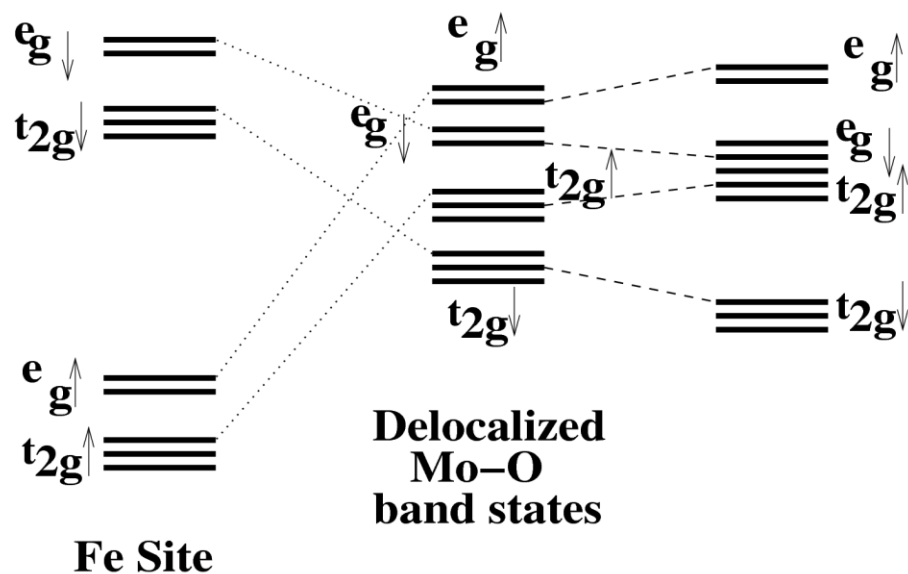


□ Counter-intuitive considering the fact that Mo is usually non-magnetic

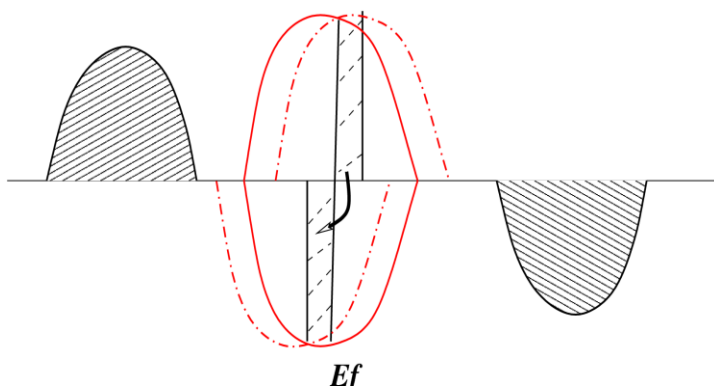
□ Exchange interaction between Fe d^5 via essentially non-mag ions is expected to AF.



Two Sublattice Double Exchange Mechanism



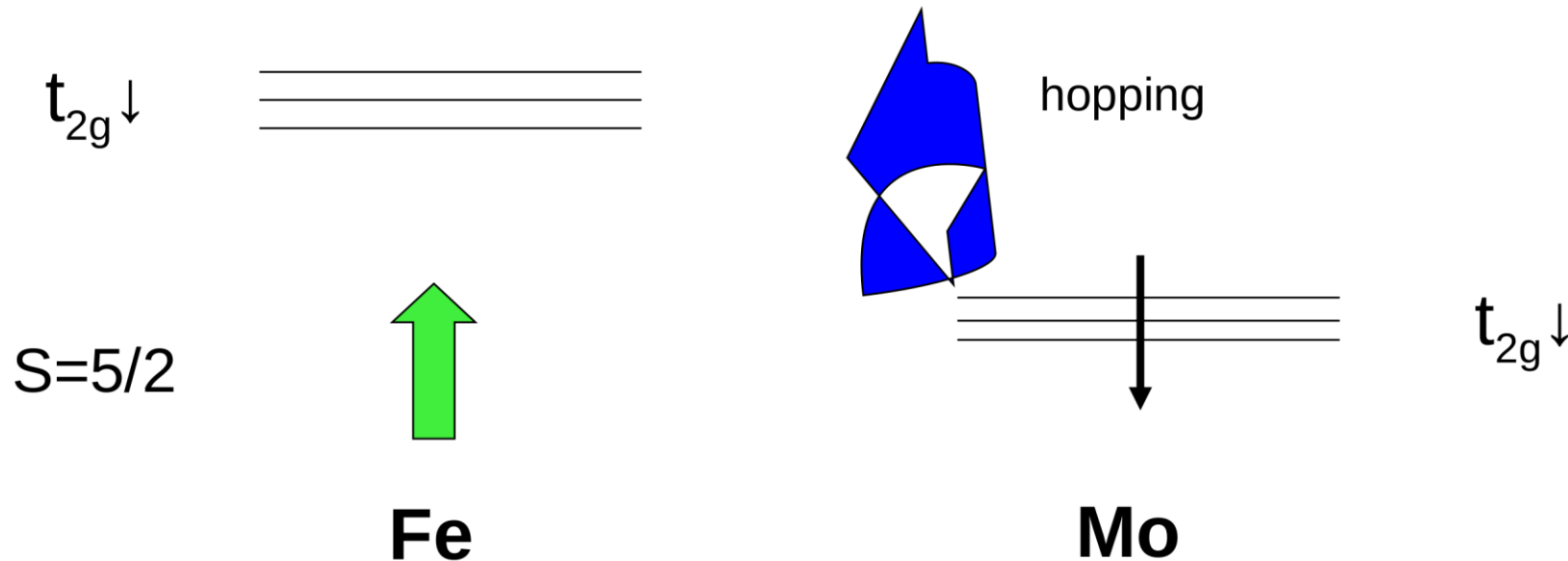
Sarma, Mahadevan, Saha-Dasgupta et. al., PRL 85, 2549



Key concept is the energy gain contributed by the negative spin polarization of the non-magn. element induced by hybridization

Effective double exchange type model Hamiltonian

- **Iron: 3d⁵:** Hund's rule: Large (classical) spin **S=5/2** : Site-localized.
- **Mo: 4d¹:** **S= -1/2**: Mobile electron: gives rise to metallic behaviour.
- Ferrimagnet: **S_{total} = 2**

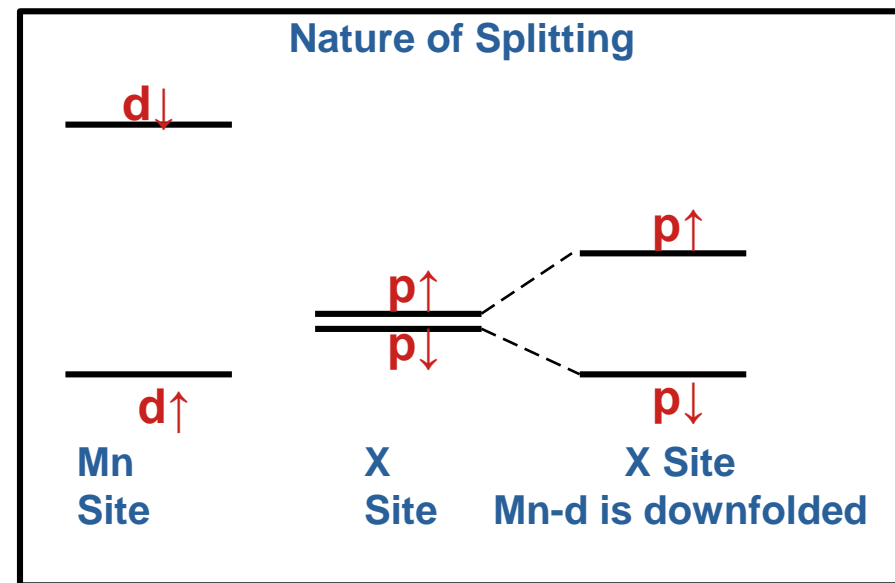
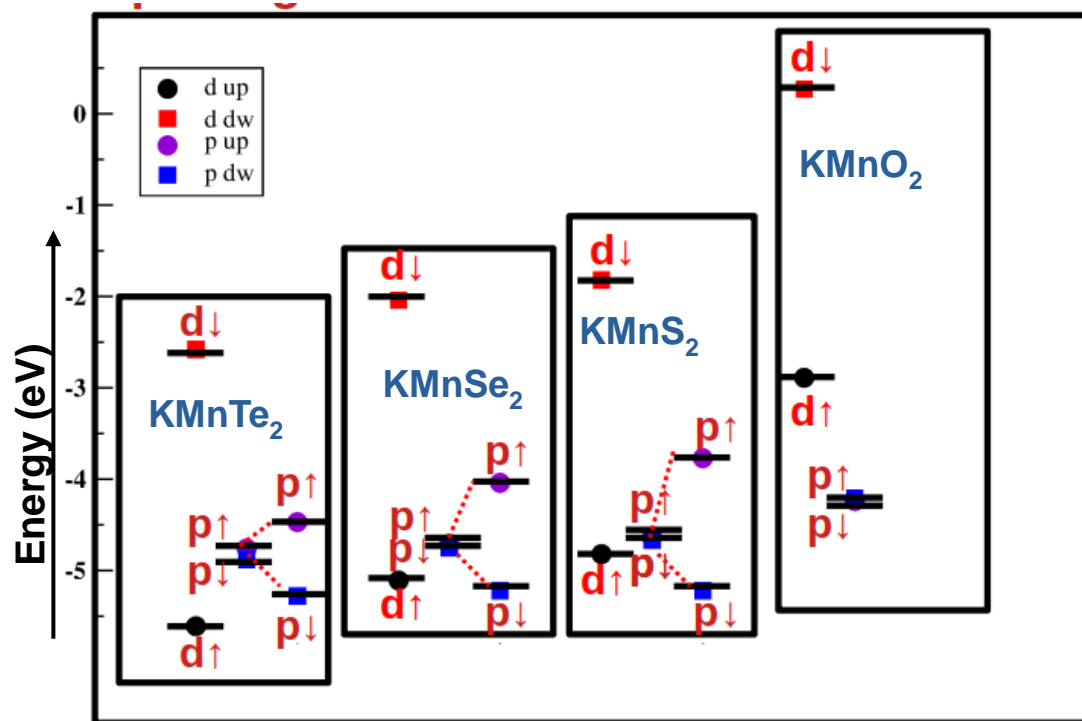


2-sublattice Kondo lattice hamiltonian :

Energy scales: t_{Fe-Mo} , $\Delta=\epsilon_{Mo}-\epsilon_{Fe}$, J

$$H = \epsilon_{Fe} \sum_{i \in A} f_{i\sigma}^\dagger f_{i\sigma} + \epsilon_{Mo} \sum_{i \in B} m_{i\sigma}^\dagger m_{i\sigma} + t_{FM} \sum_{\langle ij \rangle} (f_{i\sigma}^\dagger m_{j\sigma} + h.c.) + J \sum_{i \in A} S_i \cdot f_{i\sigma}^\dagger \sigma_{\alpha\beta} f_{j\beta}$$

Two Sublattice Double Exchange

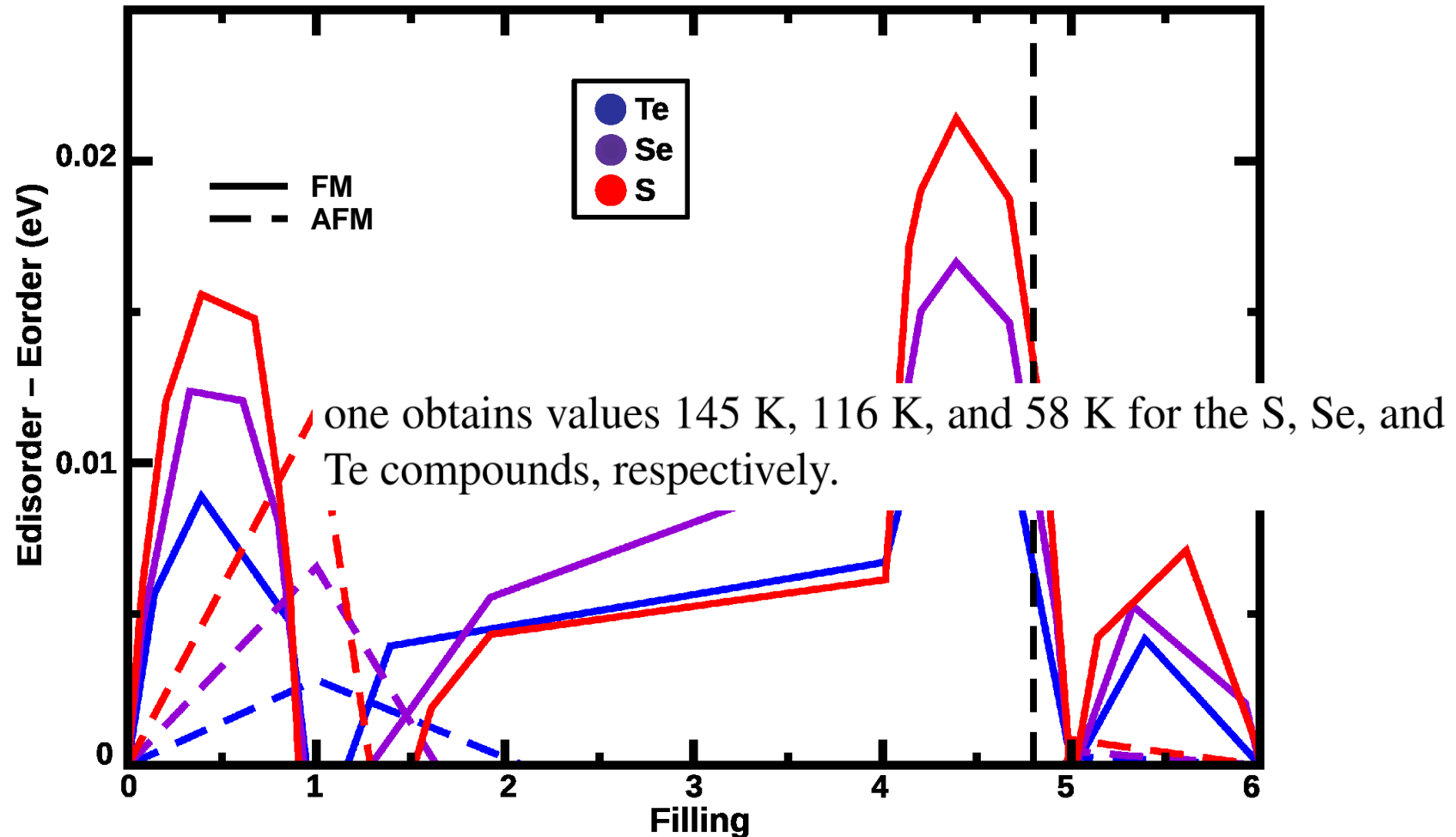


- The X-p(up) state is pushed up and the X-p(dw) state is pushed further down by the corresponding states at Mn site.
- The splitting at X site is renormalised by the large splitting at Mn site and the substantial hopping coupling between Mn and X.
- For KMnO_2 the O-p states are not between the Mn-d states, so two sublattice double exchange mechanism is not possible.

Exact Diagonalization of Model Hamiltonian

The two sublattice double exchange model Hamiltonian, considering two X atoms and one Mn atom in the basis, is thus given as follows:

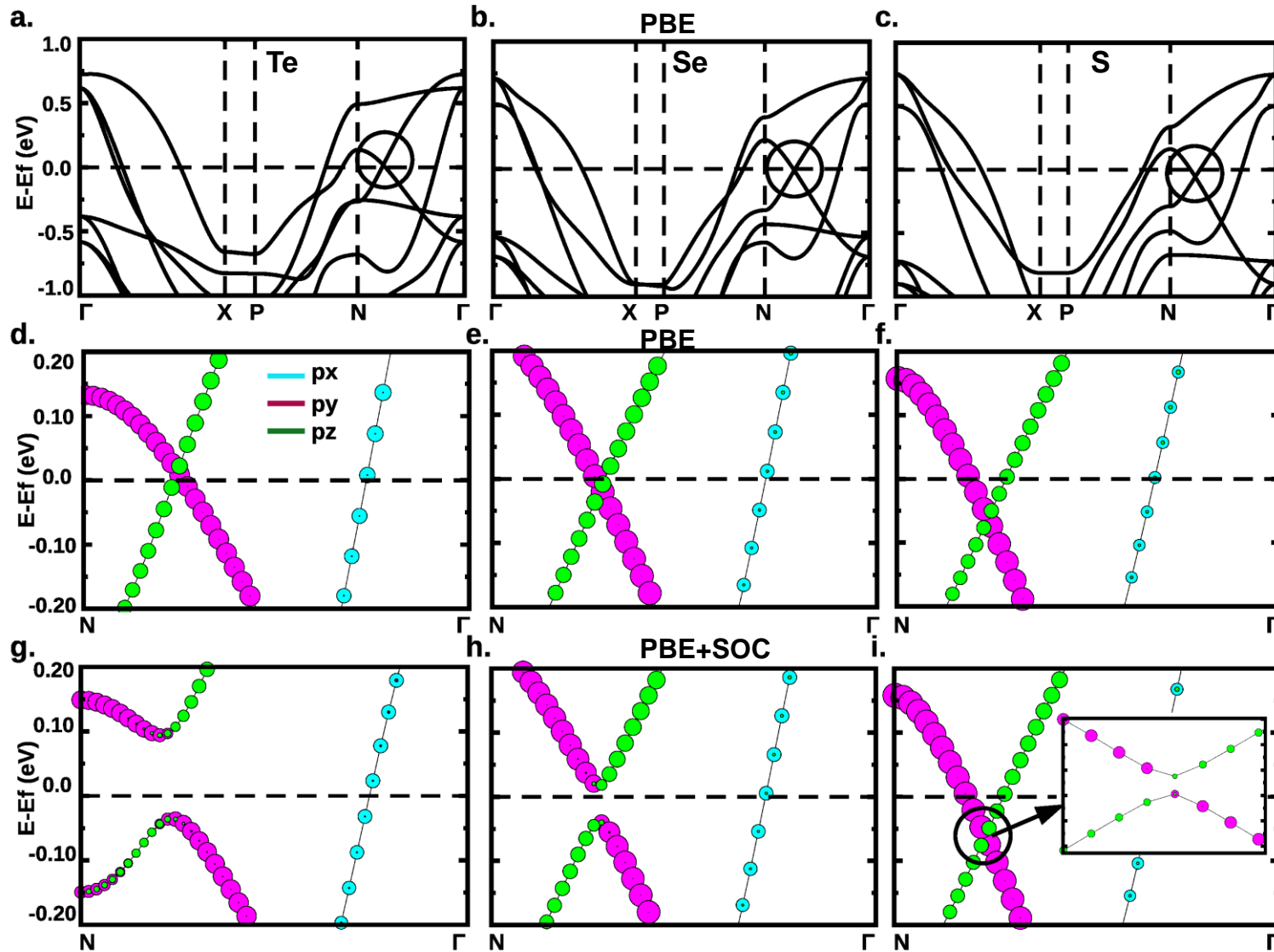
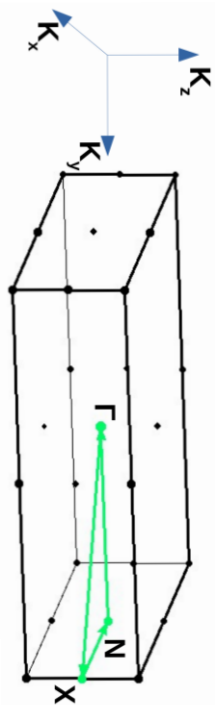
$$H = \epsilon_{Mn} \sum_{i\sigma} m_{i\sigma}^\dagger m_{i\sigma} + \epsilon_X \sum_{i\alpha\sigma} x_{i\sigma}^{\alpha\dagger} x_{i\sigma}^\alpha + t \sum_{i\delta\alpha\sigma} m_{i\sigma}^\dagger x_{i+\delta_{\alpha,\sigma}}^\alpha + J \sum_{i\mu\nu} \vec{S}_i \cdot m_{i\mu}^\dagger \vec{\sigma}_{\mu\nu} m_{i\nu}$$



➤ The filling corresponding to actual compounds is 4.8, at which all three compounds exhibit stabilization of the ferromagnetic phase.

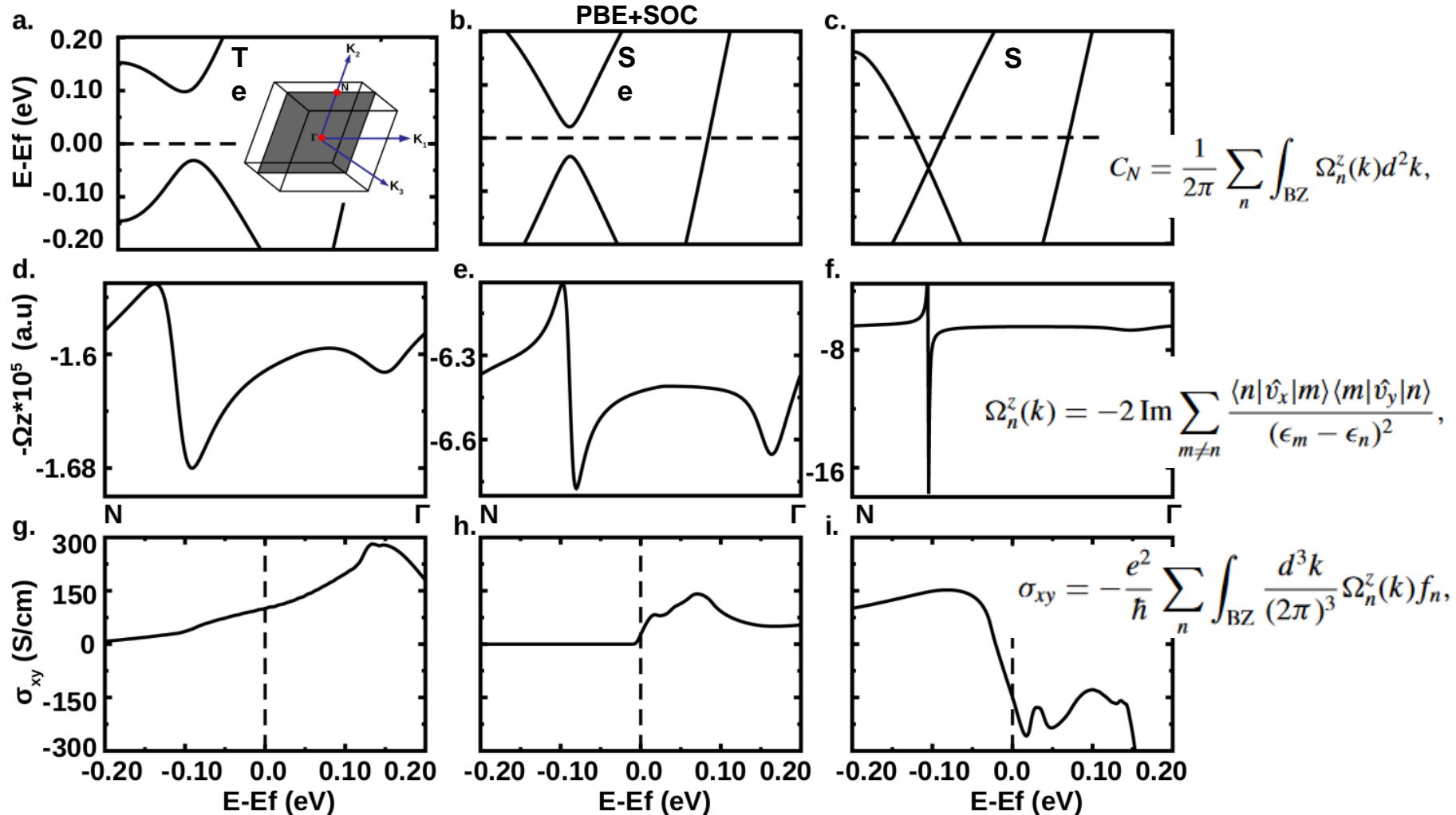
TOPOLOGICAL PROPERTIES

Band Anticrossing



- The crossing at $k=(0,0.35,0)$, between the high symmetry points N and Γ arises due to bands of two different orbital characters, p_z and p_y .
- Upon inclusion SOC, a band inversion happens, with the bands interchanging their orbital characters.
- Thus the crossing $k=(0,0.35,0)$ is an “anti-crossing” point.

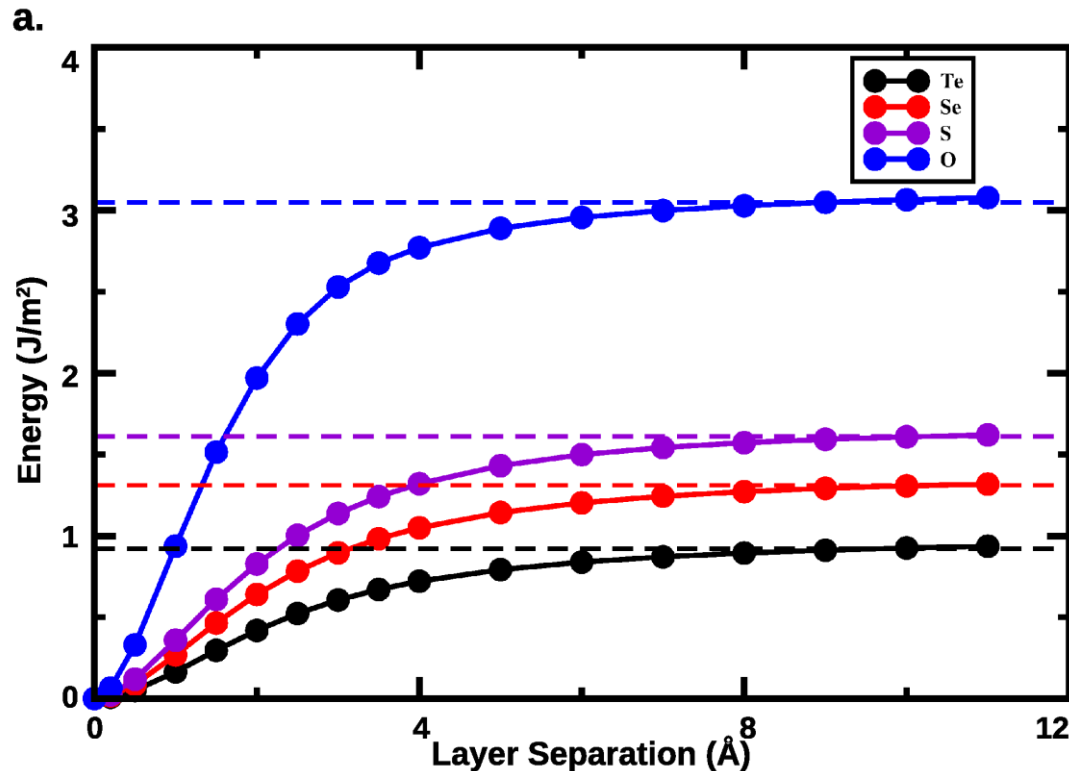
Anomalous Hall Conductivity



➤ The Chern number corresponding to the anti-crossing bands is **ONE** in each of the three compounds. Thus, the bands forming the anti-crossing, are Chern bands.

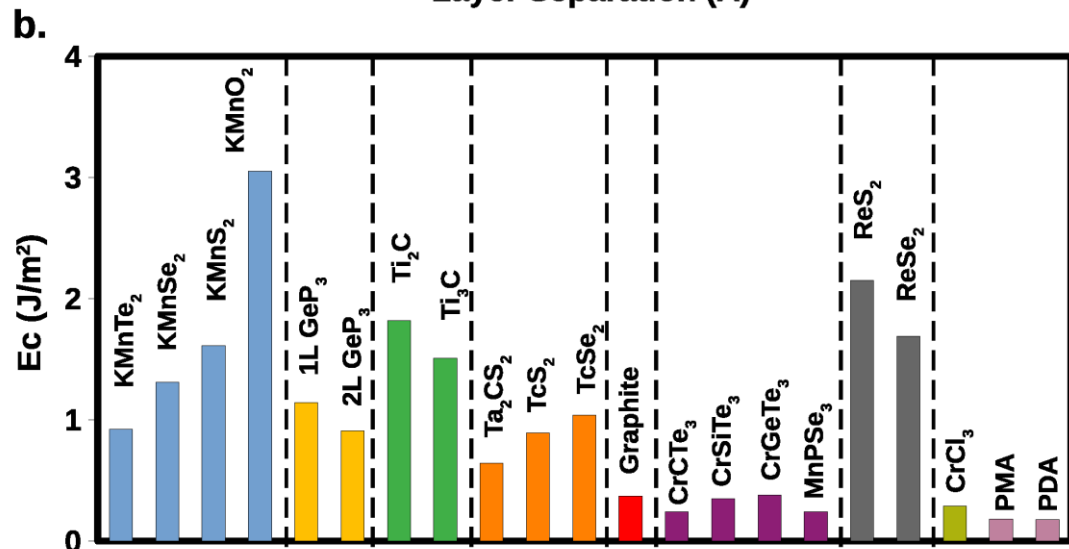
➤ Berry curvature peaks around the anti-crossing points. AHC arises solely out of the majority spin channel. Chern metal in one spin channel and insulator in other spin channel.

Monolayer limit: Cleavage Energy Calculation



The cleavage energy is the normalized energy required to generate two (top and bottom) surfaces by cleaving the bulk layered structure.[*]

$$E_{\text{cleavage}} = [E(d_{\text{sat}}) - E_{\text{g.s}}] / A$$



➤ Except KMnO_2 ($E_c = 3.05 \text{ J/m}^2$) the computed E_c values for KMnX_2 are reasonably small (0.92, 1.31, 1.61 J/m^2 for KMnTe_2 , KMnSe_2 , KMnS_2 respectively). **This strongly suggest that these compounds, except KMnO_2 , are cleavable.**

➤ These compounds are not van der Waals compounds, the 2D counterparts may be obtained through chemical etching.

➤ The magnetic ground states of the cleaved layers continued to ferromagnetic.

CONCLUSION


- **Robust half-metallicity** in these compounds is driven by two-sublattice double exchange mechanism that arises due to positioning of essentially non-magnetic $X-p$ levels within the strongly spin-split levels of Mn $S=5/2$.
- These compounds are **topological half-metals**, with a metallic character of nontrivial topology in one spin channel and an insulating character in the other spin channel.

Chern half-metals – Route to Topological Quantum Spintronics

Dimensionality reduction may open up exotic physics!

PHYSICAL REVIEW B **107**, 155115 (2023)

Robust half-metallicity and topological properties in square-net potassium manganese chalcogenides

Koushik Pradhan,¹ Prabuddha Sanyal,² and Tanusri Saha-Dasgupta ^{1,*}

¹*Department of Condensed Matter and Materials Physics, S. N. Bose National Centre for Basic Sciences, JD Block, Sector III, Salt Lake, Kolkata, West Bengal 700106, India*

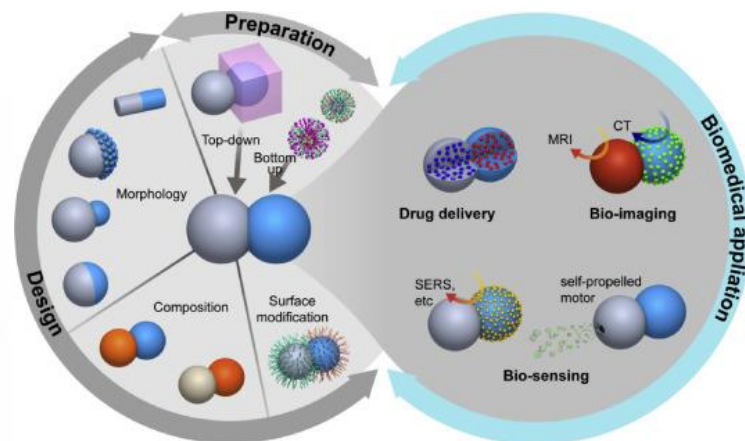
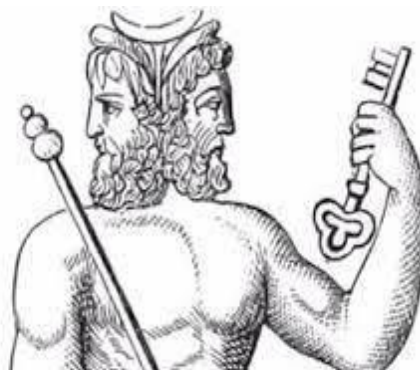
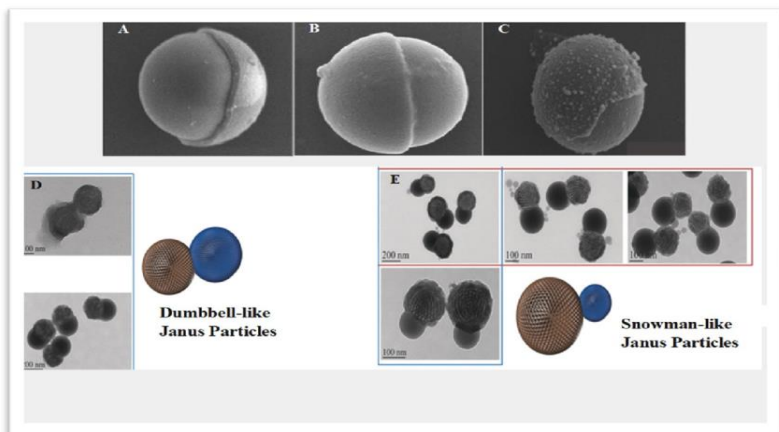
²*Department of Applied Physics, Maulana Abul Kalam Azad University of Technology, West Bengal 700064, India*



(Received 5 January 2023; revised 26 March 2023; accepted 28 March 2023; published 7 April 2023)

PART II

**Giant Rashba Effect and Non-linear Anomalous Hall
Conductivity in 2D Janus MXene**

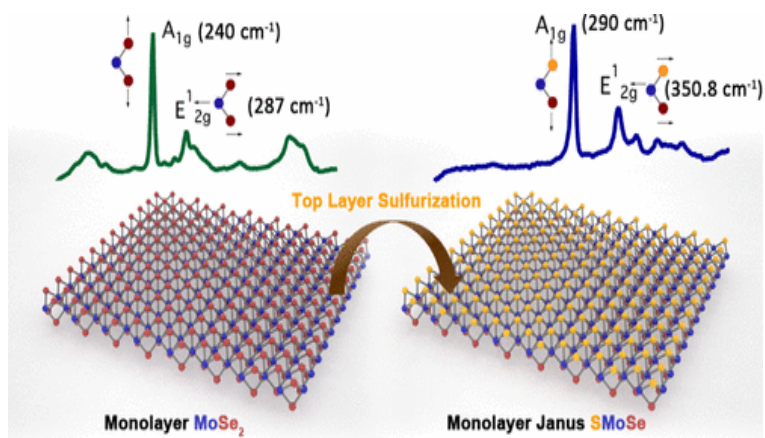


Pharmaceutics 15(2):423

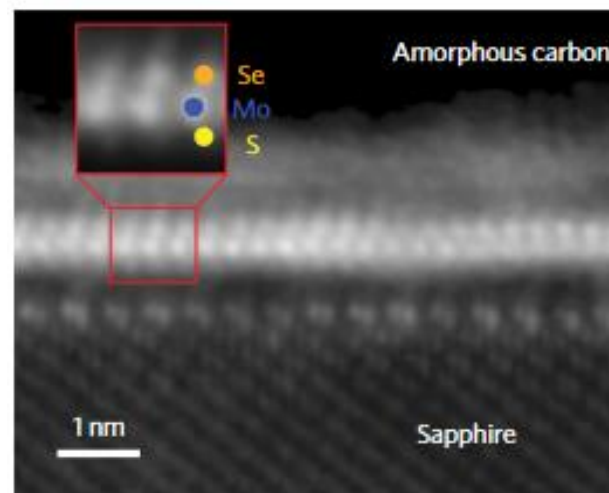
Materials Today Bio

Volume 4, September 2019,
100033

Janus 2D structures



ACS Nano 2017, 11, 8, 8192–8198



Nature Nanotechnology volume 12, pages 744–749 (2017)

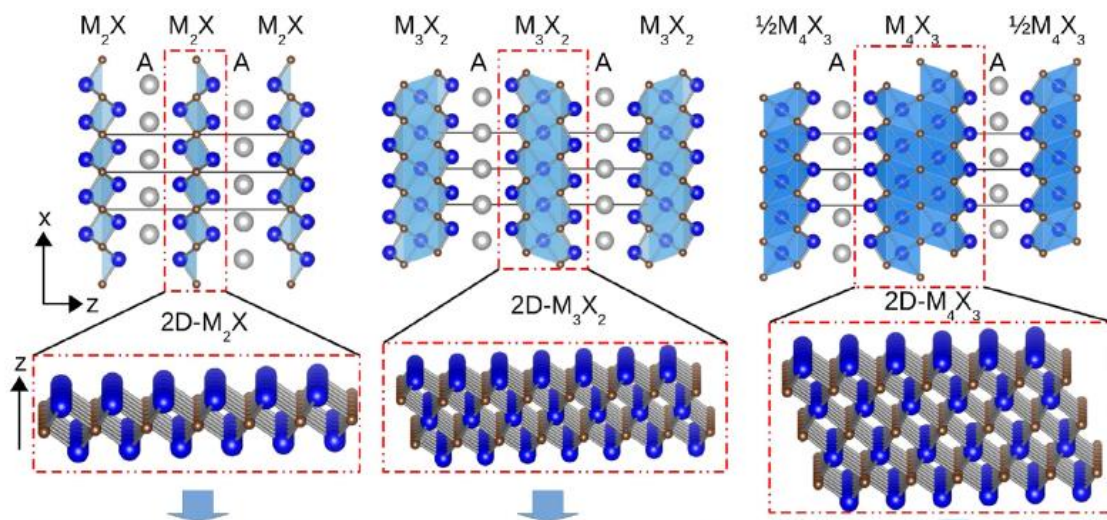
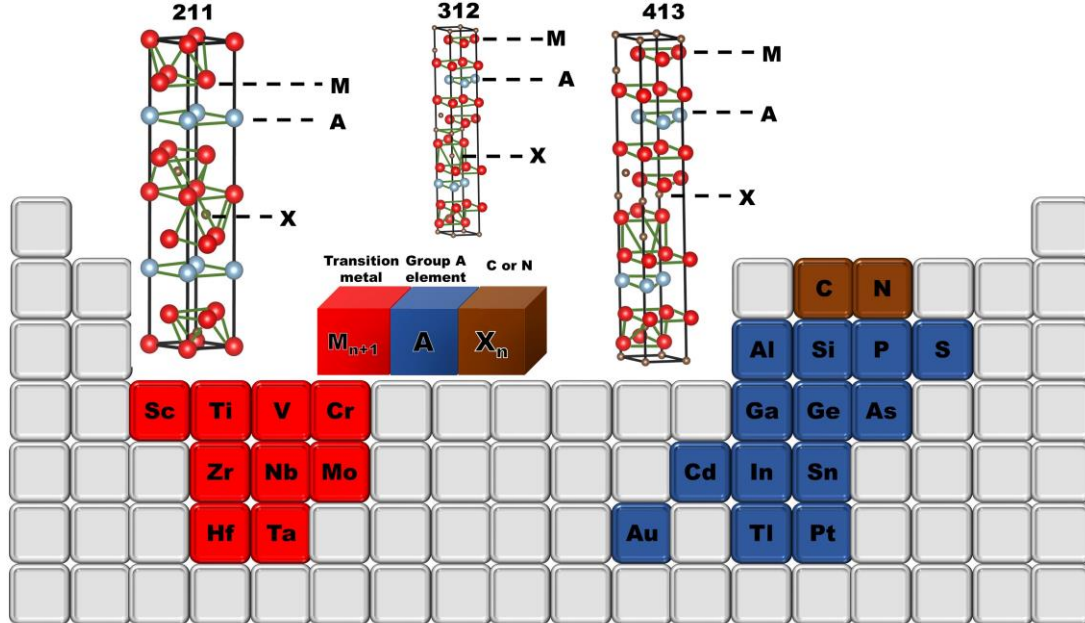
MAX and MXenes



bulletin | cover story

MAX phases: Bridging the gap between metals and ceramics

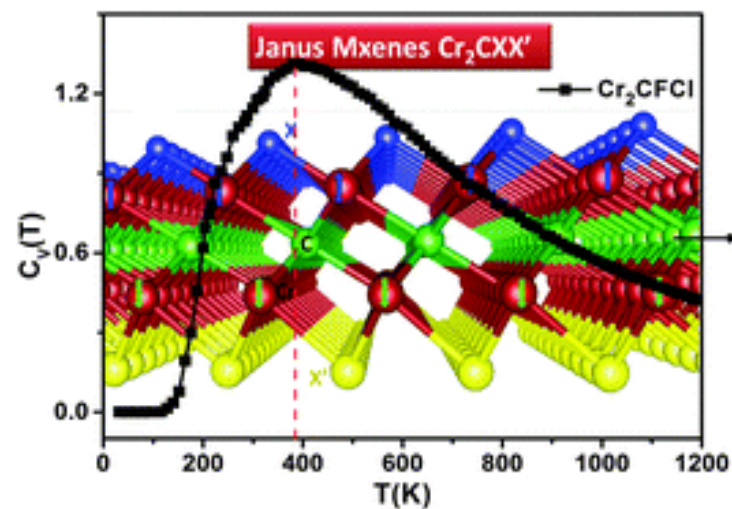
By Miladin Radovic and Michel W. Barsoum



M_2X	Synthesis	Theory
M_2C	$Ti_2C, Sc_2C, V_2C, Cr_2C, Mo_2C, W_2C, Zr_2C, Ta_2C, Nb_2C, Hf_2C$	$Ti_2C, Sc_2C, V_2C, Cr_2C, Mo_2C, W_2C, Zr_2C, Ta_2C, Nb_2C, Hf_2C$
M_2N	$Ti_2N, V_2N, W_2N, Cr_2N, Mo_2N, Zr_2N, Nb_2N, Ta_2N, Hf_2N$	$Ti_2N, V_2N, Sc_2N, Cr_2N, Mo_2N, W_2N, Zr_2N, Ta_2N, Hf_2N$
Mixed	$(Ti,V)_2C, (Ti,Nb)_2C$	$^a(Ti,V)_2C, ^a(Ti,C,B)$

M_3X_2	Synthesis	Theory
M_3C_2	$Ti_3C_2, Sc_3C_2, V_3C_2, Zr_3C_2, Mo_3C_2, Ta_3C_2, Hf_3C_2$	$Ti_3C_2, Sc_3C_2, V_3C_2, Cr_3C_2, Zr_3C_2, Mo_3C_2, Nb_3C_2, Ta_3C_2$
M_3N_2	$^aTi_3N_2, ^aTa_3N_2$	$Ti_3N_2, ^aSc_3N_2, ^aV_3N_2, Cr_3N_2, Ta_3N_2, Nb_3N_2, Zr_3N_2$
Mixed	$(Ti,V)_3C_2, (Cr,V)_3C_2, (Ti,Cr)_3C_2, (V,Mo)_3C_2, (Ti,Mo)_3C_2, ^a(Ti,V)_3C_2, ^a(Ti,C,B)$	$(Ti,Ta)_3C_2, (Ti,Cr)_3C_2, (Ti,Nb)_3C_2, (Ti,Mo)_3C_2, (V,Mo)_3C_2, (V,Cr)_3C_2, (Nb,Cr)_3C_2, (Ta,Mo)_3C_2, (Ta,Cr)_3C_2, (Nb,Mo)_3C_2, ^a(Sc,Mo)_3C_2$

M_4X_3	Synthesis	Theory
M_4C_3	$^aTi_4C_3, ^aV_4C_3, Nb_4C_3, Ta_4C_3$	$Ti_4C_3, ^aSc_4C_3, V_4C_3, ^aMo_4C_3, Zr_4C_3, Nb_4C_3, Ta_4C_3$
M_4N_3	$Ti_4N_3, ^aV_4N_3, Ta_4N_3$	$Ti_4N_3, Sc_4N_3, ^aV_4N_3, ^aCr_4N_3$
Mixed	$(Ti,Nb)_4C_3, (Ti,Mo)_4C_3, (Zr,Nb)_4C_3$	$(Ti,V)_4C_3, (Ti,Ta)_4C_3, (Ti,Nb)_4C_3, (Ti,Cr)_4C_3, (Ti,Mo)_4C_3, (V,Cr)_4C_3, (Nb,Ta)_4C_3, (Nb,Cr)_4C_3, (Nb,Mo)_4C_3, (Mo,Ta)_4C_3, (Cr,Ta)_4C_3$

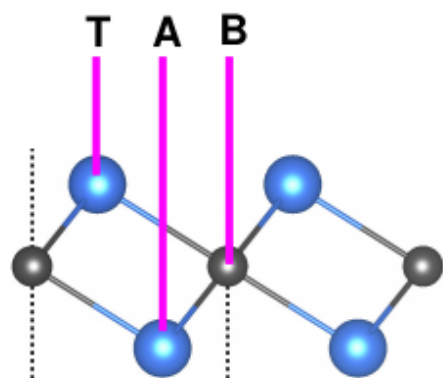


Chakraborty, Das & Saha-Dasgupta

J. Mater. Chem. C, 2016, 4, 6500-6509

Comprehensive Nanoscience and Nanotechnology (Second Edition)

A.

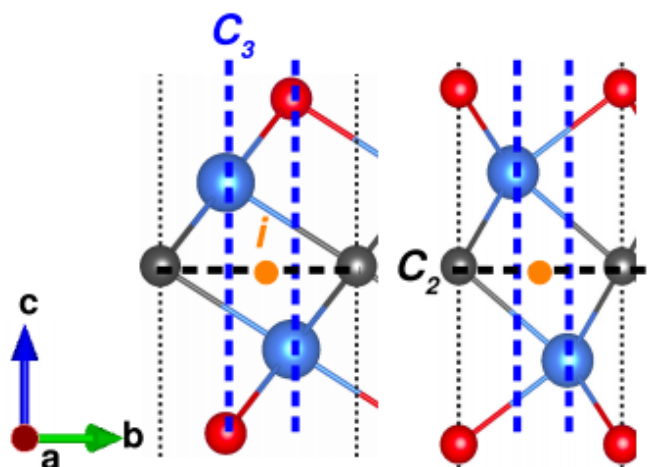


B.

Symmetric MXene

AA

BB

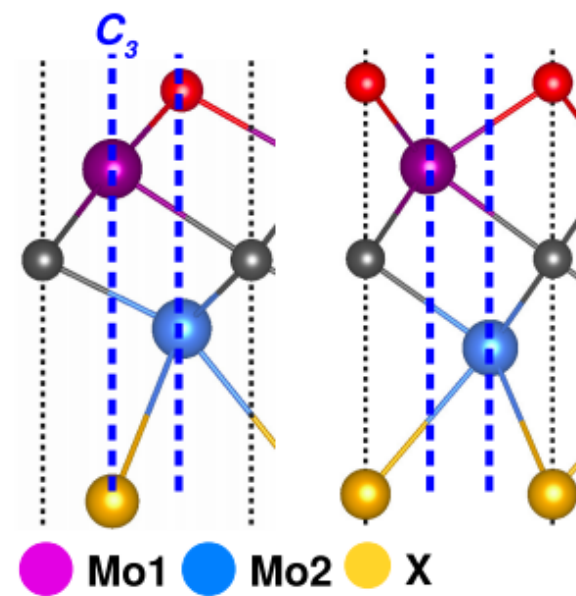
P $\bar{3}m1$

C.

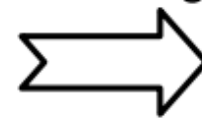
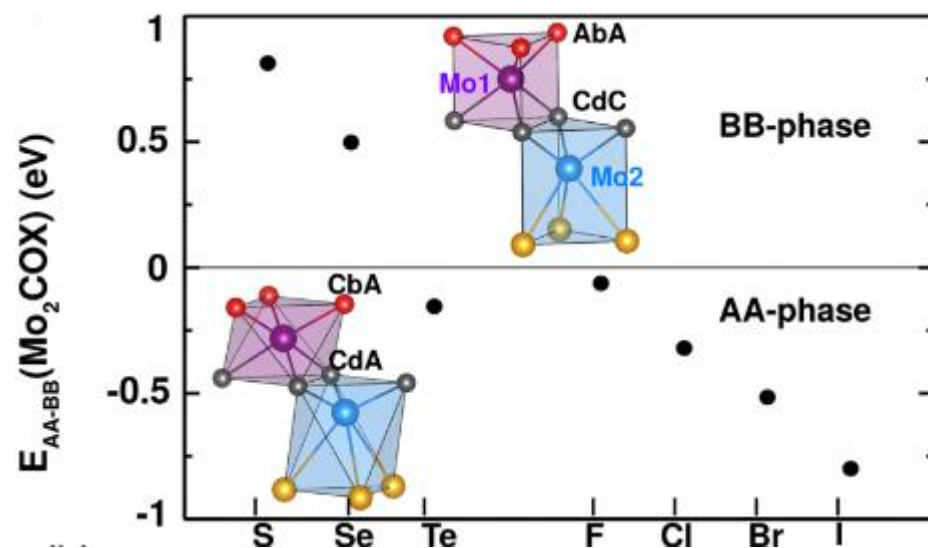
Janus MXene

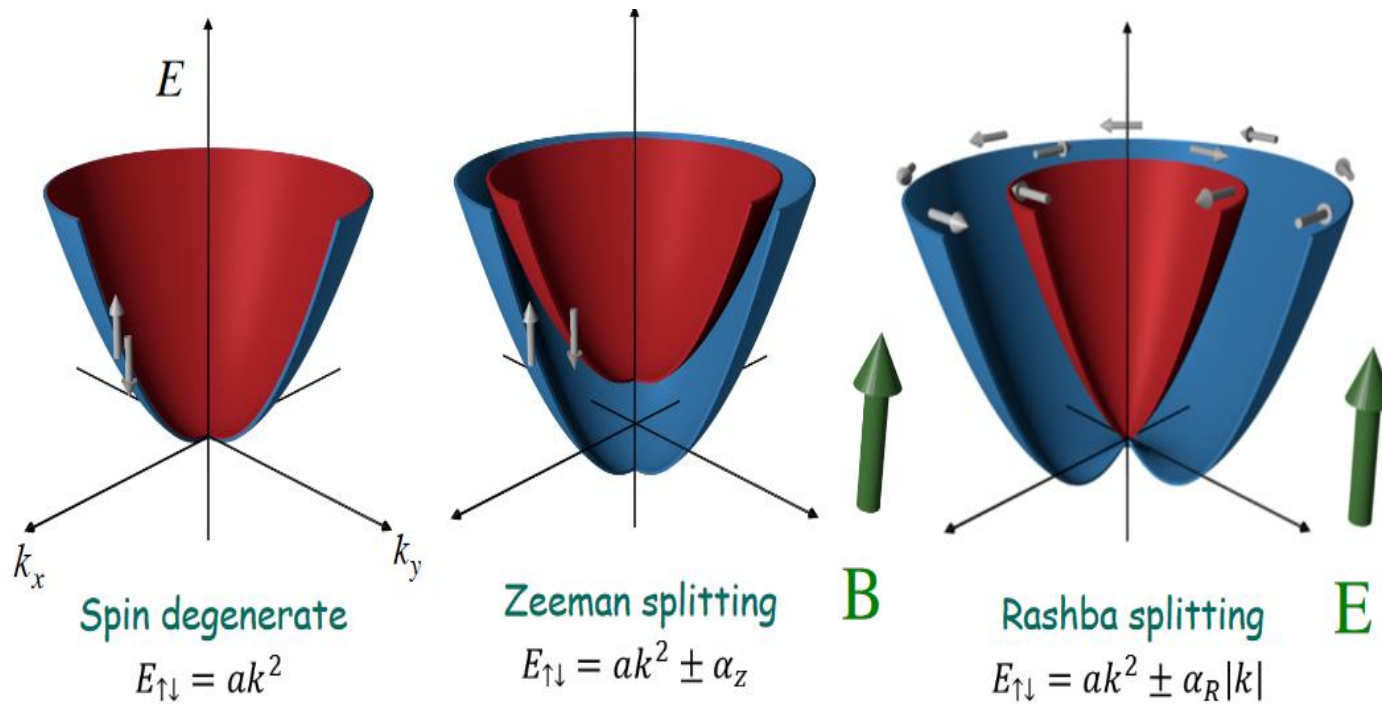
AA

BB



P3m1

Inversion
symmetry
breakingX: S, Se, Te
F, Cl, Br, IBroken Inversion Symmetry
+
Strong SOC



Emmanuel I. Rashba (1927-)

Ref: Rashba, Sov. Phys. Solid State (1960)

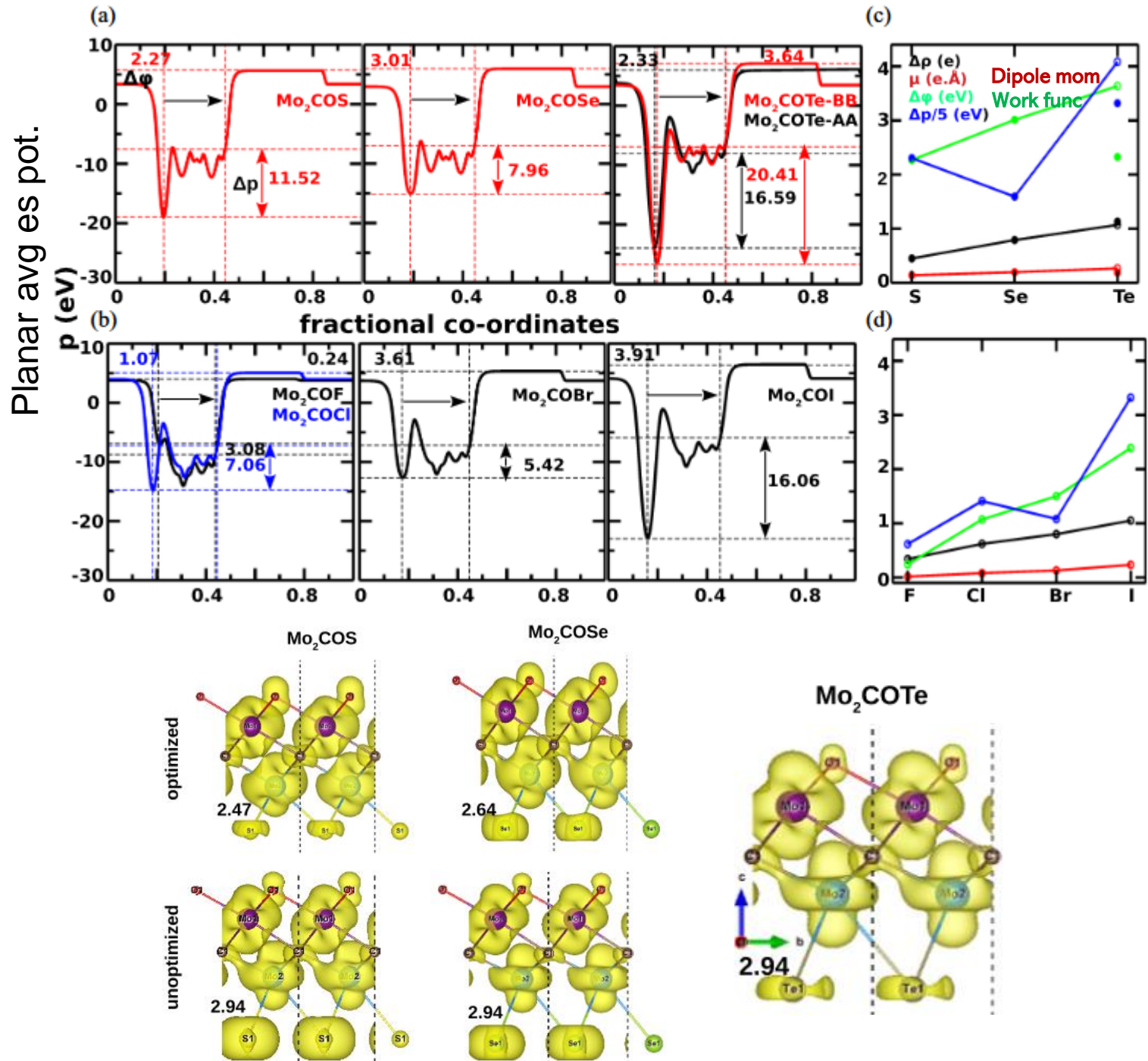
- a. TR & IR symmetry intact
- b. TR broken , IR intact
- c. TR intact , IR broken

The momentum-dependent spin splitting (2DEG) subjected to a perpendicular electric field

$$H_R = \alpha_R (k_y \sigma_x - k_x \sigma_y)$$

$$\epsilon_k = (\hbar^2 k^2 / 2m^*) \pm \alpha_R k$$

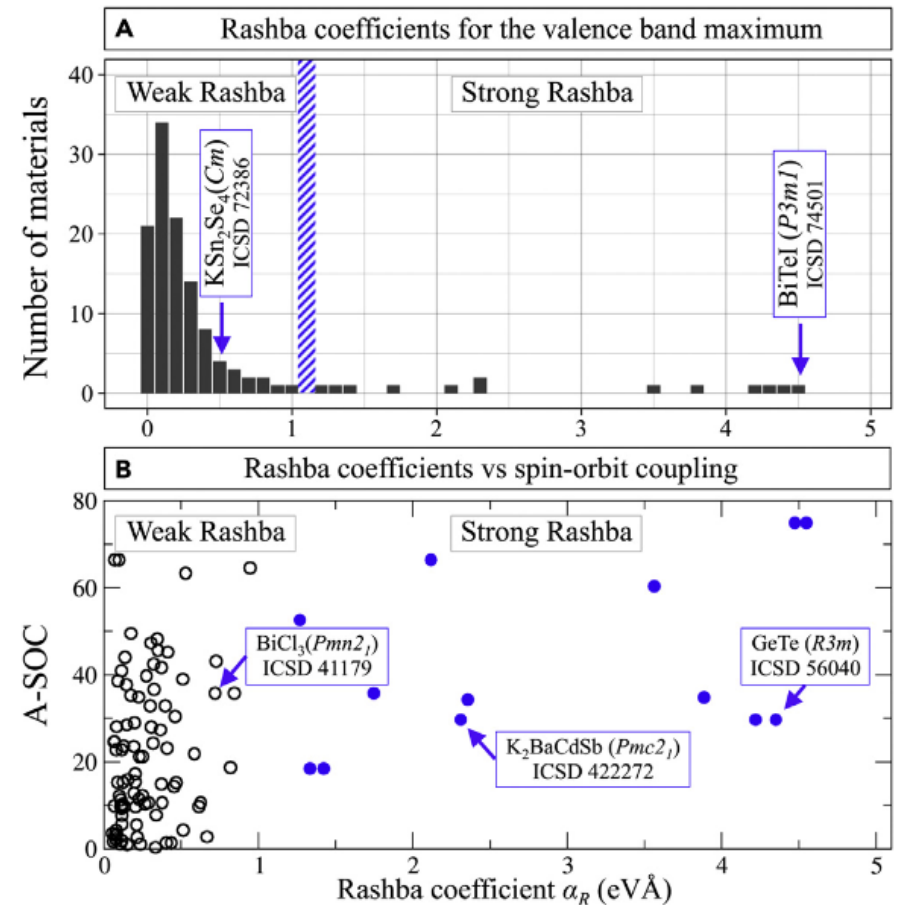
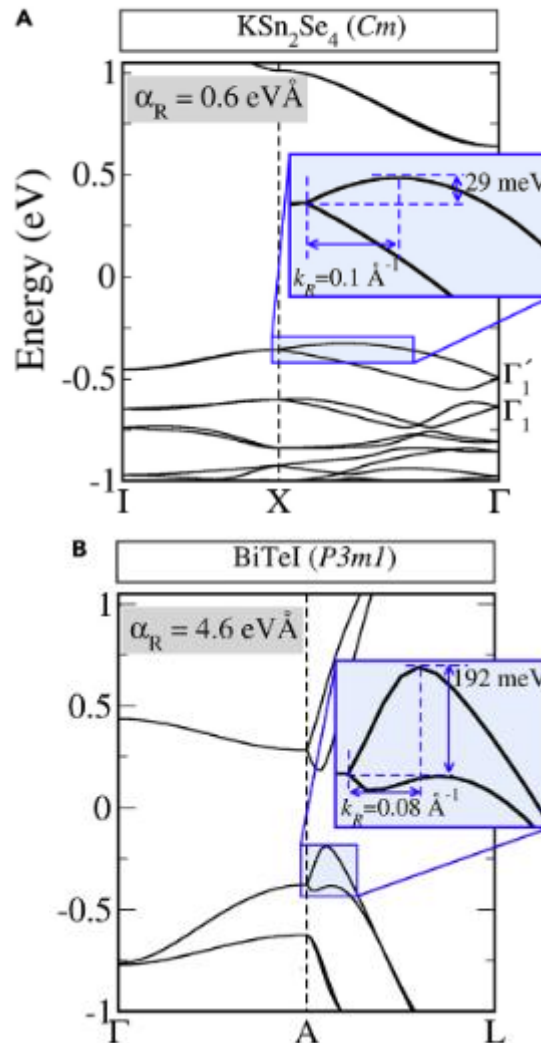
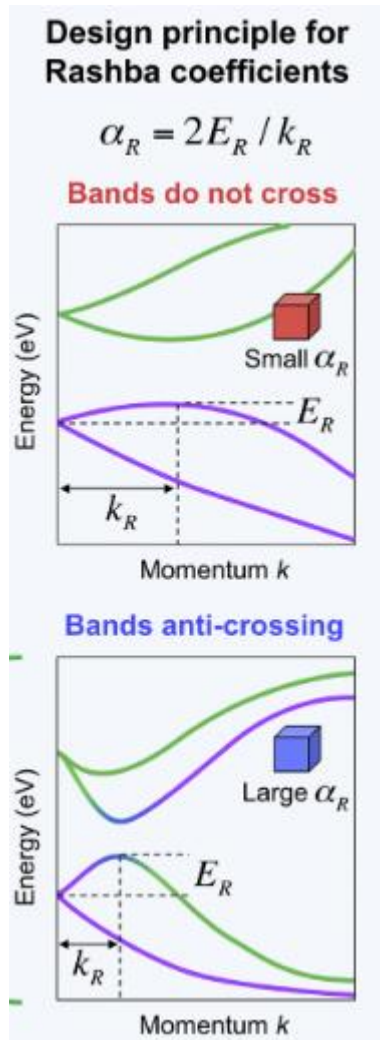
Polarization Properties

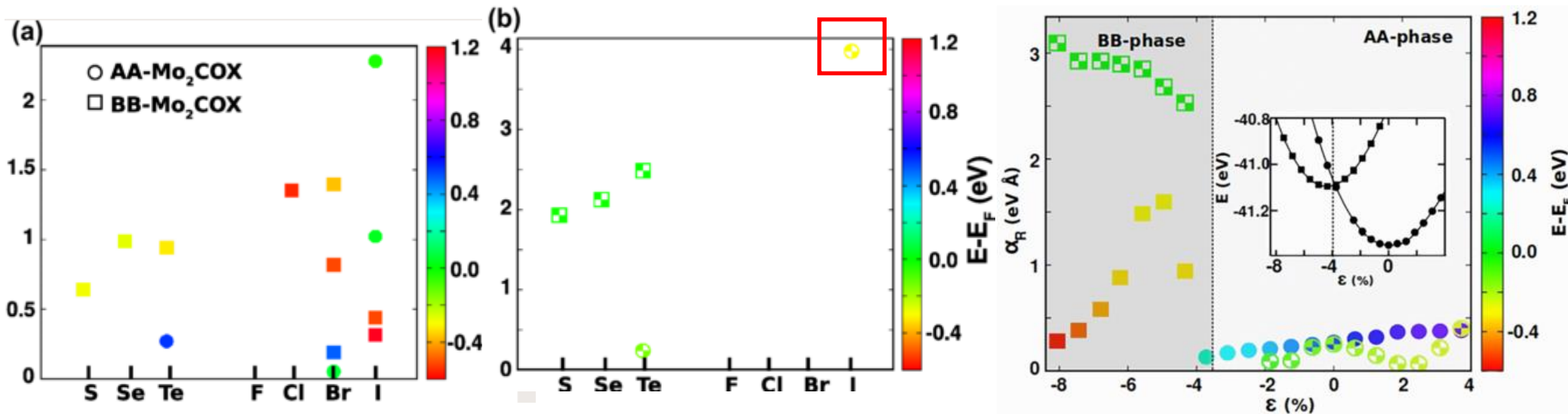
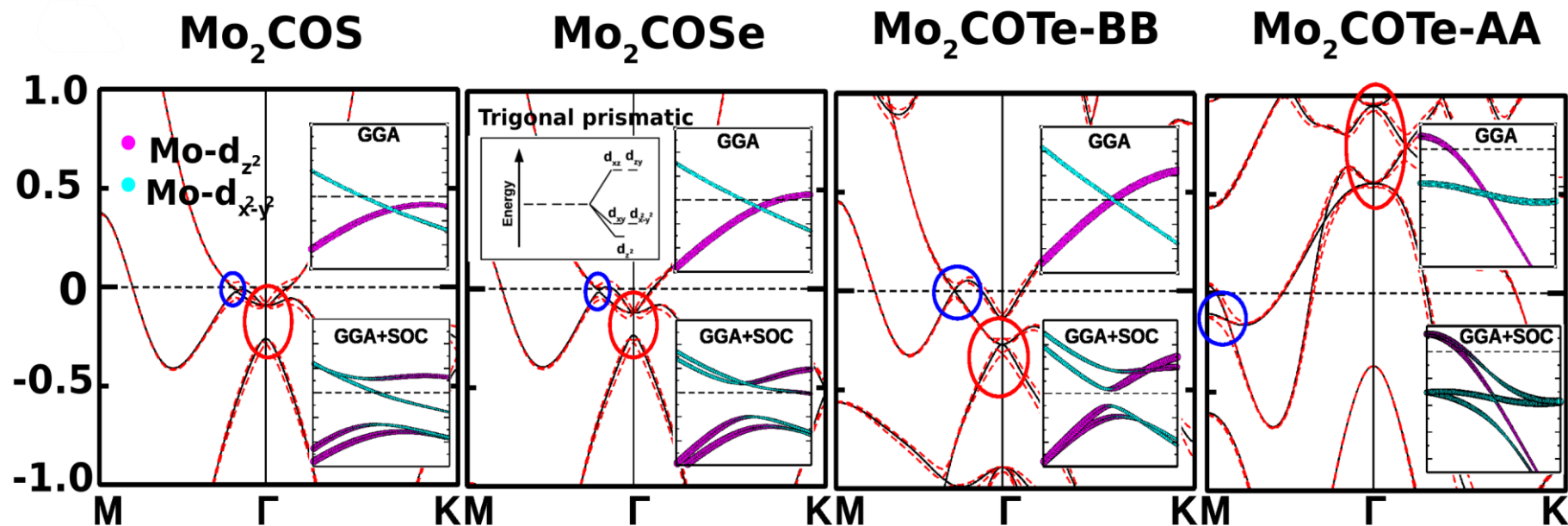


The Rashba Scale: Emergence of Band Anti-crossing as a Design Principle for Materials with Large Rashba Coefficient

Carlos Mera Acosta, Elton Ogoshi, Adalberto Fazzio, Gustavo M. Dalpian, Alex Zunger

Matter 3, 145-165 (2020)





Strong Rashba compounds ($\geq 1.0 \text{ eV \AA}$)

TRS ✓ Linear response regime, AHE vanishes

Non-linear Response

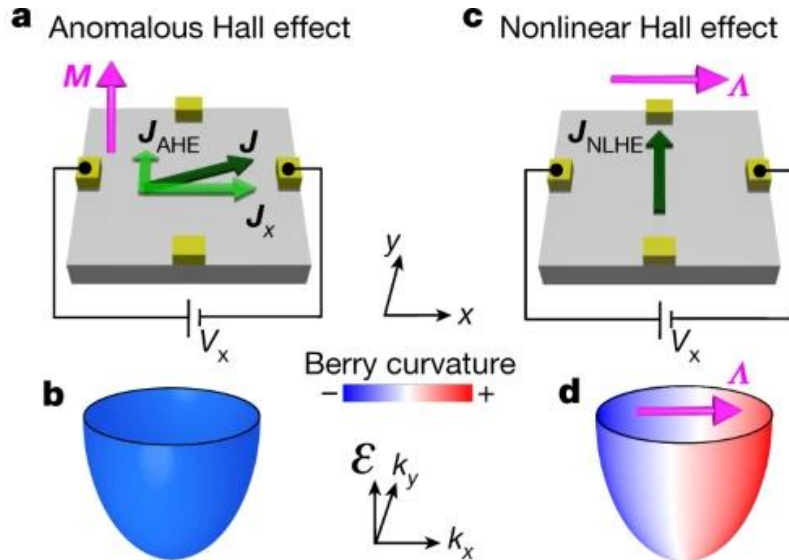
$$\Omega^n(k) = -\Omega^n(-k) \quad \text{Berry curvature is ODD}$$

TRS ✓
Inversion ✗

Non-Linear response regime,
2nd order Hall effect (NAHE) Berry curvature dipole

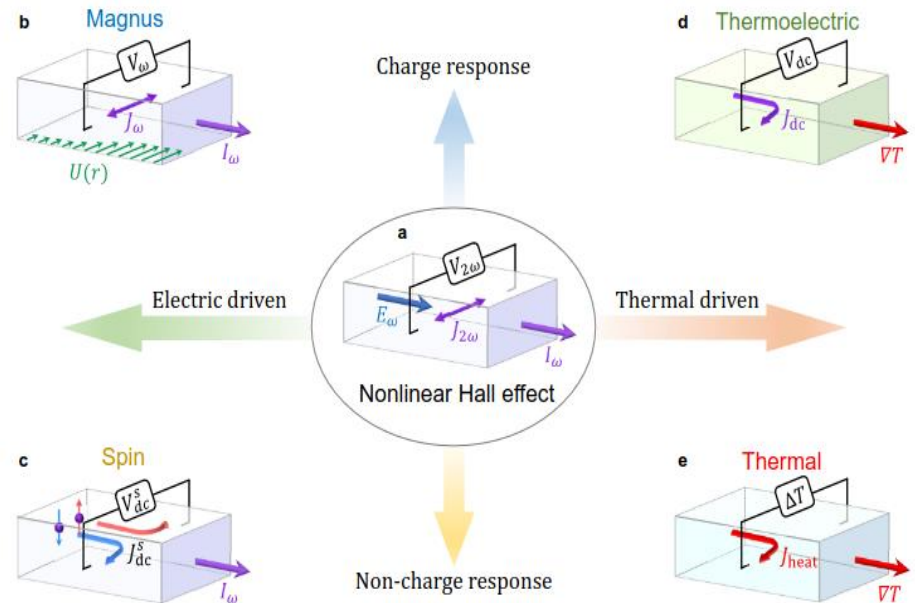
– quadratic Hall voltage

$$J_a = \sigma_{ab} E_b + \chi_{abc} E_b E_c + \dots$$



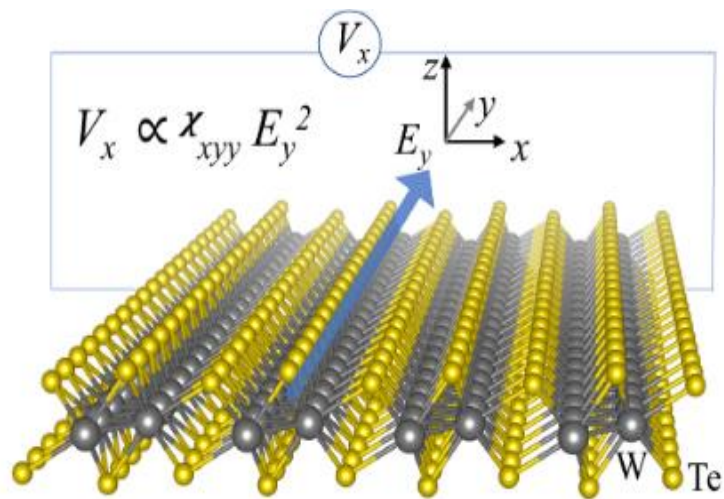
Observation of the nonlinear Hall effect under time-reversal-symmetric conditions

Nature **565**, 337–342 (2019)



Perspective: Nonlinear Hall Effects

Z. Z. Du,^{1,2} Hai-Zhou Lu,^{1,2,*} and X. C. Xie^{3,4,5}

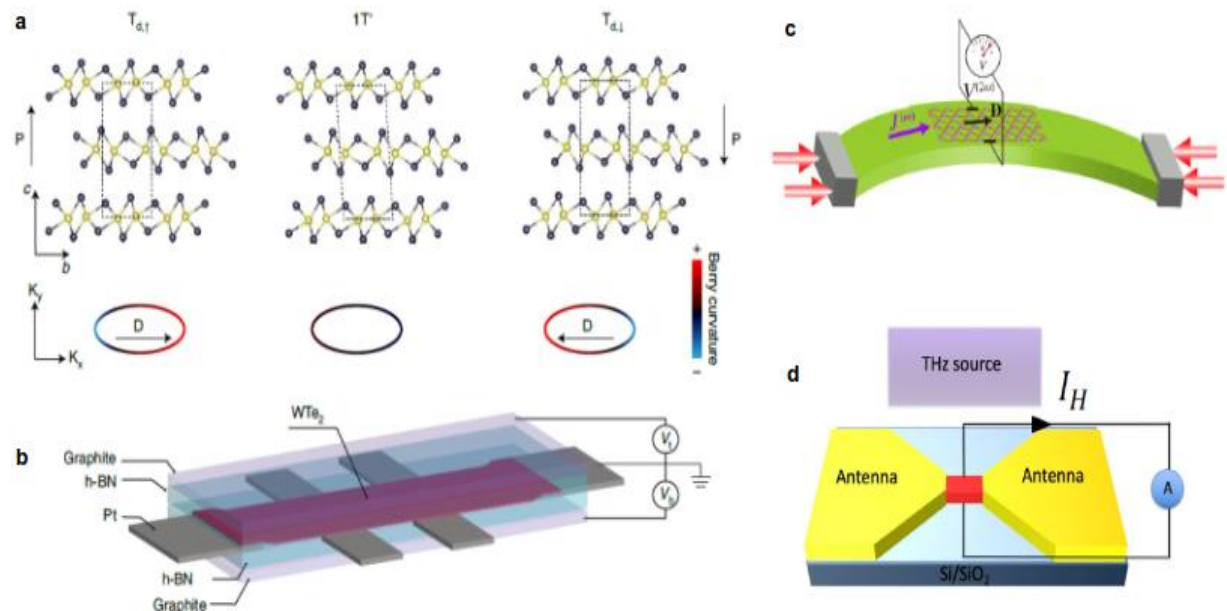


2D Mater 5, 044001

Can one achieve NAHE in absence of external field ?

Experiments on non-linear Hall effect

Materials	Dimension	Temperature (K)	Input current frequency (Hz)	Input current maximum (μA)	Output voltage maximum (μV)	Carrier density (cm^{-2} in 2D, cm^{-3} in 3D)
Bilayer WTe ₂ [24]	2	10-100	10-1000	1	200	$\sim 10^{12}$
Few-layer WTe ₂ [25]	2	1.8-100	17-137	600	30	$\sim 10^{13}$
Strained monolayer WSe ₂ [40]	2	50-140	17.777	5	20	$\sim 10^{13}$
Twisted bilayer WSe ₂ [42]	2	1.5-30	4.579	0.04	20000	$\sim 10^{12}$
Corrugated bilayer graphene [41]	2	1.5-15	77	0.1	2	$\sim 10^{12}$
Bi ₂ Se ₃ surface [45]	2	2-200	9-263	1500	20	$\sim 10^{13}$



Applications:

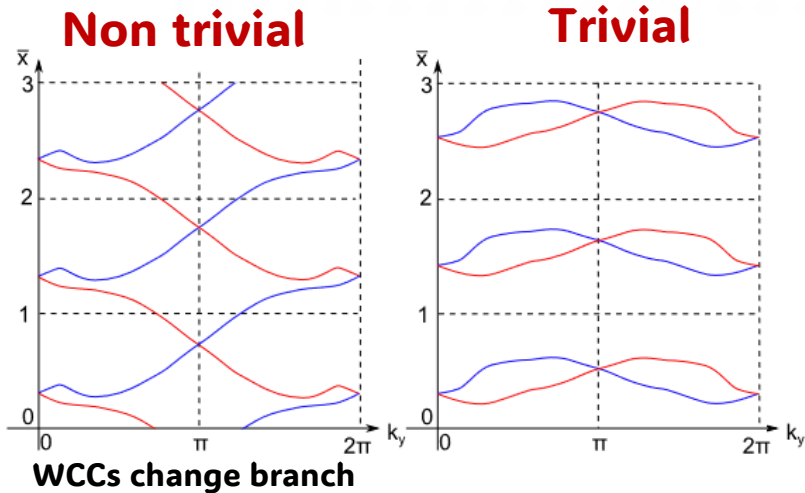
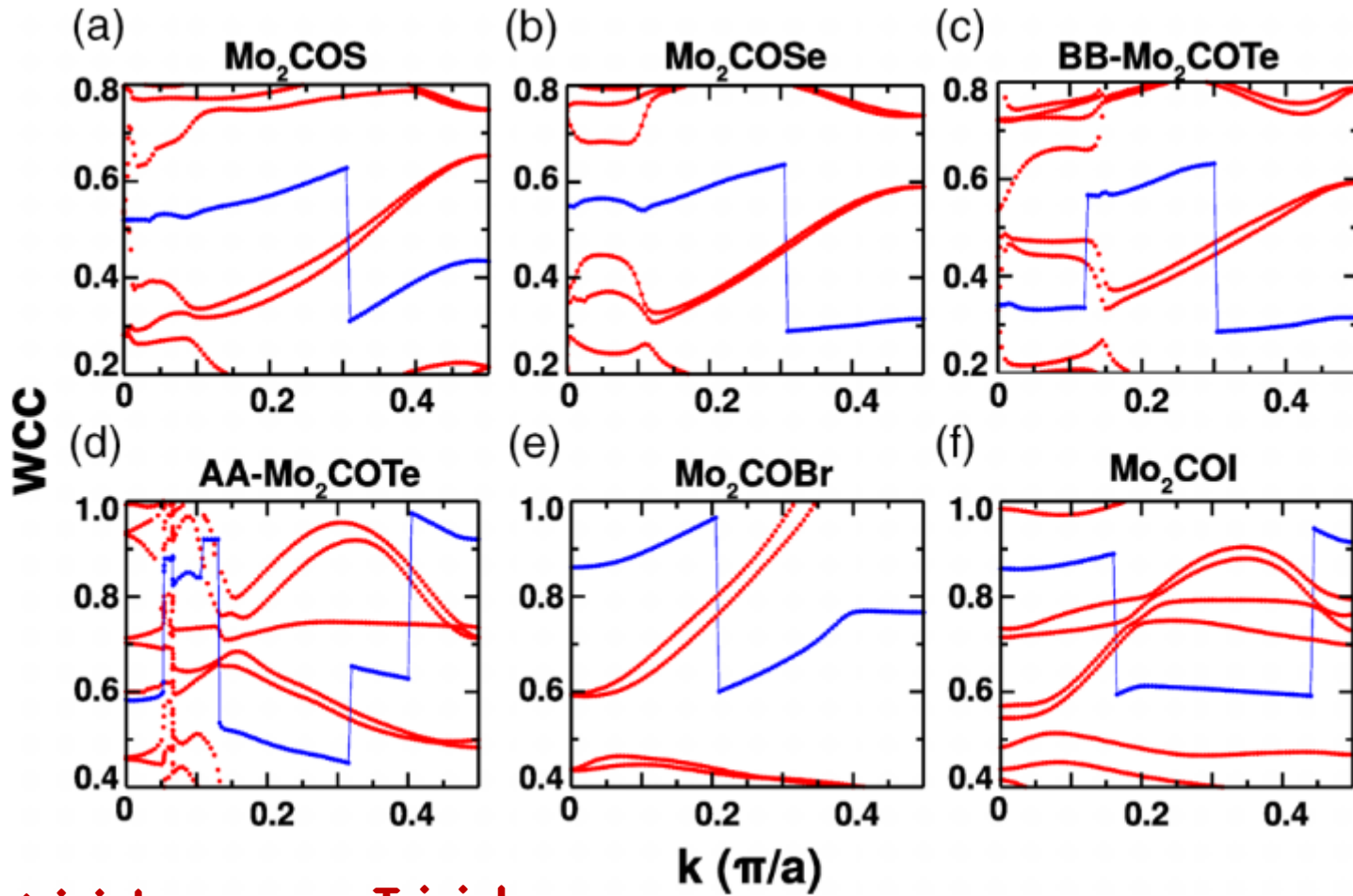
- Berry curvature memory device
- Piezoelectric device
- Photo detection device

Nonlinear Hall effects

Z. Z. Du, Hai-Zhou Lu & X. C. Xie

Nature Reviews Physics 3, 744–752 (2021)

Evolution of Wannier Charge Centers along TR-invariant plane $kz=0$ line

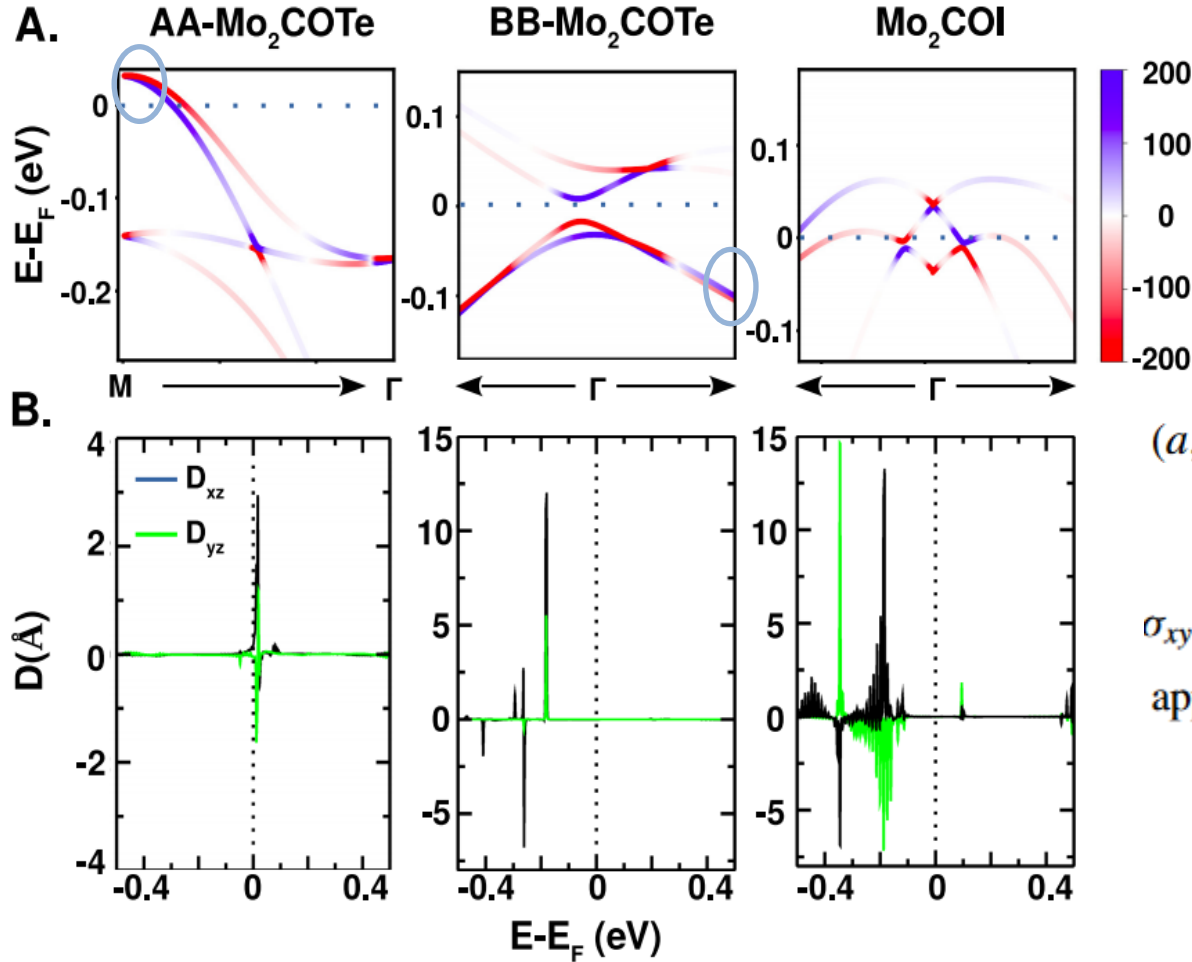


$$\nu = \# \text{ discontinuities of } z(k_y) \text{ in } [0, \pi] \pmod{2}.$$

The interspace fn intersects
WCCs even no of times

Topologically TRIVIAL





Compound	D_{xz} (Å)	position w.r.t E_F	σ_{xy} 10^{-4} (G_0)	D_{yz} (Å)	position w.r.t E_F	σ_{yx} 10^{-4} (G_0)
AA-Mo ₂ COTe	2.946	+0.017	14.098	-1.634	0.011	7.820
BB-Mo ₂ COTe	12.014	-0.179	57.482	5.516	-0.181	26.393
Mo ₂ COI	13.272	-0.184	63.504	14.634	-0.345	70.019

$$\chi_{abb} = -\varepsilon_{adb} \frac{e^3 \tau}{2\hbar^2 (1 + i\omega\tau)} D_{bd}$$

($a, b = x, y$ and $d = z$)

$$D_{bd} = \int_{\mathbf{k}} f_n^0(\mathbf{k}) \frac{\partial \Omega_d^n}{\partial k_b},$$

$$\sigma_{xy} = \chi_{yxx} E_x = (e^3 \tau / \hbar^2) D_{xz} = G_0 \tau \bar{D}_{xz} e E_x \pi / \hbar$$

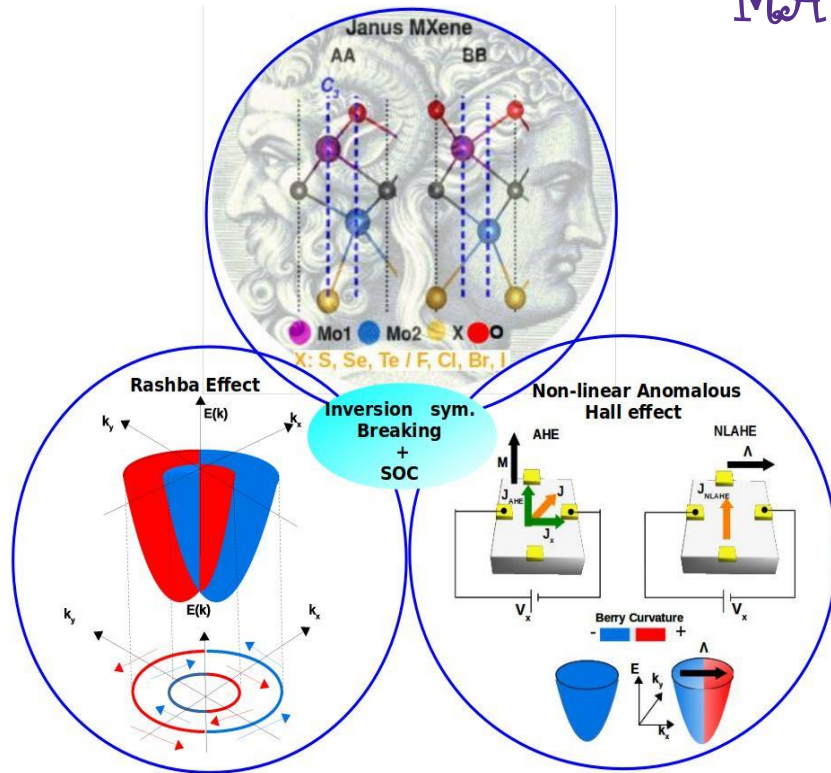
applied field $E_{y/x} = 10^3$ V/m $\tau = 10^{-12}$ s

$$G_0 = 2e^2 / h$$

$$1T' - WTe_2 (\sigma_{xy} \approx 0.005 G_0)$$

CONCLUSION - II

COMPOSITE QUANTUM MATERIALS



**Application in
spintronics devices
through interface
engineering**

**Berry curvature
memory device**

PHYSICAL REVIEW B

covering condensed matter and materials physics

Highlights Recent Accepted Collections Authors Referees Search Press About Editorial Team

Giant Rashba effect and nonlinear anomalous Hall conductivity in a two-dimensional molybdenum-based Janus structure

Shiladitya Karmakar, Rajdeep Biswas, and Tanusri Saha-Dasgupta
Phys. Rev. B **107**, 075403 – Published 6 February 2023